Automated Optimization under Dynamic Flow Conditions
Supporting Information

Table of Contents

Table of Figures

Table of Tables

Analytical Methods:

HPLC Analysis:

Samples were collected at fixed time intervals throughout the preliminary and optimization experiments for offline HPLC analysis in order to obtain reaction understanding and generate an FTIR chemo-metric model. During preliminary experiments, samples were collected every minute, leveraging a sampling interval protocol requiring 30 seconds of collection, followed by 30 seconds of waste. For the optimizationexperiments, the sampling frequency was reduced as these samples were to be leveraged to verify the optimization-driving FTIR results. Additionally, given the extended duration of the optimization experiments (~1000 minutes), an every minute sampling protocol was deemed excessive. For optimization experiment #1, samples were collected every three minutes (intervals: collection = 30 seconds, waste = 150 seconds) whereas, for optimization experiment #2, samples were collected every twelve minutes (intervals: collection = 60 seconds, waste = 660 seconds).

HPLC analysis was leveraged during initial experimentation in an effort to establish a feasible operating region from a reaction kinetics perspective as well as a reference result for the calibration and generation of an FTIR predictive model. After FTIR model validation, HPLC was leveraged sparingly as an orthogonal analytical tool to confirm predicted concentration results and trends during the automated optimization runs. All HPLC results were obtained using an Agilent 1290 Infinity II instrument (and associated software) equipped with an Agilent ZORBAX Eclipse Plus C18 (50 mm x 4.6 mm, 1.8 µm particle size) column. A fit-for-purpose gradient HPLC method was adapted from a method reported previously [1] for this particular chemistry application. Method details are provided in the table below.

Table S1. Chromatographic Conditions for all HPLC analyses

Column:	Agilent ZORBAX Eclipse Plus C18 (50 mm x 4.6 mm, 1.8 µm particle size)	
Detector:	UV at 220 nm; Response: 40 Hz	
Temperature:	20°C	
Flow rate:	1.0 mL/min	
Injection Volume: Needle Wash:	2 µL Acetonitrile	
Sample Tray Temperature:	20°C	
Mobile Phase:	A: 0.1% H_3PO_4 in Water	
	B: Acetonitrile	
Mobile Phase Program:	Time (min)	% B
	0.0	50
	2.0	50
	3.5	95
	4.4	95
	4.5	50
	6.5	50 *(built in post-time)*

Approximate Retention Times

Name	RT (min)
4,4'-(4-nitro-1,3-phenylene)dimorpholine	1.14
4-(3-fluoro-4nitrophenyl)morpholine	1.38
2,4-Difluoronitrobenzene	1.57
4-(5-fluoro-2-nitrophenyl)morpholine	1.69
Biphenyl	4.29
Bibenzyl	4.70

Preparation of Solutions

In preparation for analysis, 4 µL of reaction sample from each fraction is diluted with 1 mL pure acetonitrile.

Prior to each run, 2 µL of the starting material solution (~1.25M 2,4-difluoronitrobenzene in ethanol) was diluted with 1 mL pure acetonitrile to confirm concentration. Additionally, to allow for quantification of the flow ratio (and, by association, the realized equivalents) of the morpholine (2) relative to the 2,4-difluoronitrobenzene (1) streams, a solution of 0.5 mL (1) + 0.5 mL (2) was mixed, a 4 uL aliquot taken and diluted in 1 mL acetonitrile, and analyzed to quantify the ratio between internal standards knowing the concentration of each stream.

Analysis

Calibration curves were generated using known standards to extract response factors for each of the species within the linear region. To enable calibration, 2,4-difluoronitrobenzene was obtained from Aldrich, 4,4'-(4-nitro-1,3-phenylene)dimorpholine and 4-(5-fluoro-2-nitrophenyl)morpholine were obtained from AmBeed, and 4-(3-fluoro-4-nitrophenyl)morpholine was procured from Accela, and were all used as-received. Biphenyl and Bibenzyl were procured from Sigma-Aldrich and Aldrich, respectively, and were used as-received.

Results were analyzed in bulk with a few key data transformations. To account for error associated with sample preparation (pipetting, dilution) and sample injection volumes, all species area counts were normalized leveraging the biphenyl internal standard area counts to ensure consistency across the dataset. To predict the experienced morpholine equivalents for a given sample fraction, *i*, the ratio of biphenyl to bibenzyl area counts was quantified and compared to a known value based on concentrations (see Equation S1).

$$\mathrm{Eq}iv_{\mathrm{Morpholine,\ i}} = \left[\frac{C_{Morpholine}}{C_{2,4\text{ - }difluoronitrobenzene}}\right]\left[\frac{\left(\frac{\mathrm{A_{Bibenzyl}}}{\mathrm{A_{Biphenyl}}}\right)_{\mathrm{i,\ Experimental}}}{\left(\frac{\mathrm{A_{Bibenzyl}}}{\mathrm{A_{Biphenyl}}}\right)_{\mathrm{Calibration}}}\right] \quad \text{(Eq. S1)}$$

All area count responses were converted to solution concentrations leveraging the above stated response factors to enable evaluation of mass balance closure, calibration of the FTIR for predictive quantification, and facilitate kinetic modeling efforts.

A few example chromatograms are provided in **Figure S1** below.

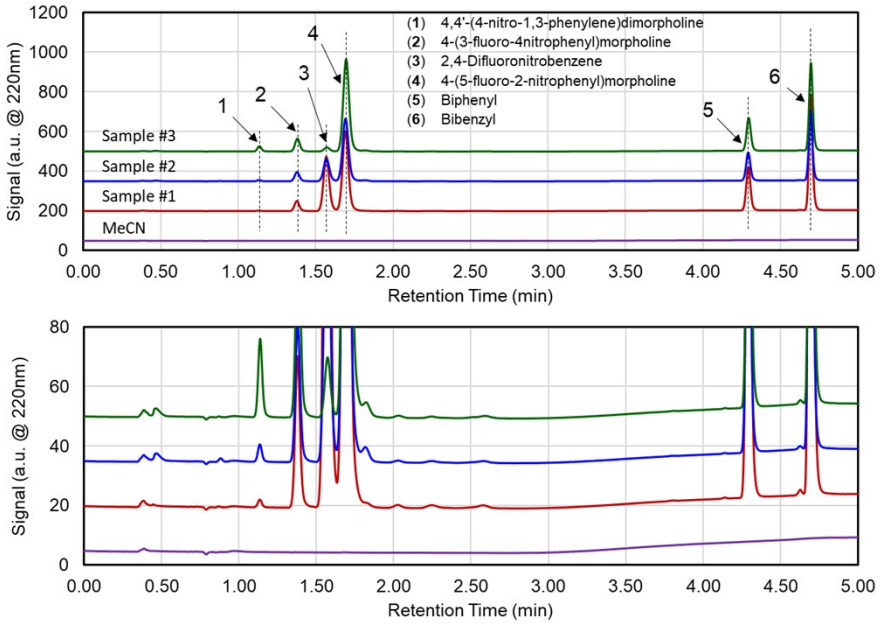

Figure S1. HPLC traces of pure solvent along with reaction samples showing the four reaction species and two internal standards. The bottom figure portrays the HPLC spectra as a close-up.

FTIR Analysis:

Principal to success of the as-designed automated optimization platform was an accurate, predictive in-line analytics model. The platform leveraged an in-line MettlerToledo ReactIR 702L equipped with a D-Sub Micro Flow Cell DiComp to record the IR spectra at 1-minute sampling intervals. The impact of scan rate was initially explored during model generation bearing in mind a desire to balance reliable model predictabilty and rapid reaction analysis. One-minute scan times were deemed sufficient for this specific chemistry application given the observed accuracy of the predictive model. Analyses of the spectra (and predictive model outputs) were performed within the Mettler Toledo iC IR software environment (version 7.1). A background spectrum was taken in air prior to each experiment and was regularly to previously obtained spectra to ensure consistency across experiments.

The iC Quant portion of the iC IR software was leveraged for the generation of a predictive multivariate model. No mathematical manipulations (i.e., 1st or 2nd derivative) were performed on the spectral set prior to use in iC Quant. The useful spectral information was restricted to two regions, 3800 – 2500 cm^{-1} and 1800 – 750 cm^{-1}. Approximately 370 data points, from initial experiments investigating the reaction performance using one-dimensional dynamic experiments as well as initial tests of the dynamic design of experiments (DDoEs), were utilized to build the multivariate model. To facilitate the model calibration, the program was allowed to leave 1 sample out in its analysis and auto-select the number of factors chosen for the fit. The final model results are shown below in **Table S2**. Parity plots comparing experimental versus predicted results are shown in **Figure S2**.

Table S2. FTIR model results and information

Species	# of Factors	RMSEC	RMSECV	RMSEP	$R^2_{cumulative}$ (training)	$R^2_{cumulative}$ (test)
2,4-difluoronitrobenzene	12	0.00401	0.00434	0.0155	0.999	0.988
4,4'-(4-nitro-1,3-	12	0.000731	0.00811	0.00289	0.997	0.987

phenylene)dimorpholine						
4-(3-fluoro-4nitrophenyl)morpholine	12	0.000584	0.000617	0.00221	0.998	0.999
4-(5-fluoro-2-nitrophenyl)morpholine	12	0.00481	0.00516	0.00996	0.998	0.999
Biphenyl	N/A[#]					
Bibenzyl	12	0.00222	0.00244	0.00463	0.999	0.985

[#] As the 2,4-difluoronitrobenzene represents the stream basis by which other stream flowrates are set, the biphenyl (which is an inert species in this reaction) concentration was unvaried throughout the set of experiments.

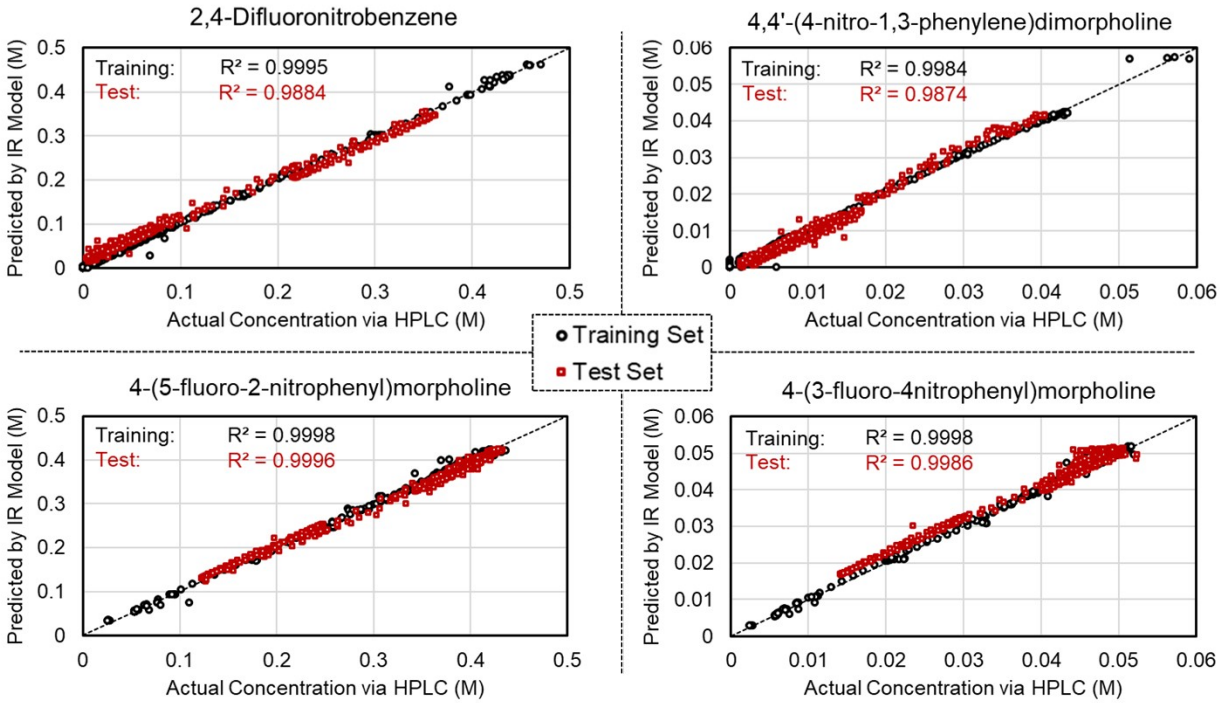

Figure S2. Parity plots comparing the actual and predicted concentration results for the four reaction species of interest.

Materials:

2,4-difluoronitrobenzene (99%) and bibenzyl (ReagentPlus, 99%) were ordered from Aldrich and used as-received. Morpholine (ACS Reagent, ≥ 99.0%), biphenyl (ReagentPlus, 99.5%), ethanol (Pure 200 proof, for molecular biology), and trifluoroacetic acid (HPLC grade, ≥99.0%) were obtained from Sigma-Aldrich and used as-is. For HPLC analyses, acetonitrile (Optima® LC/MS grade, 0.1 micron filtered) and water (UHPLC-MS grade) were purchased from Fisher and phosphoric acid was obtained from Aldrich (85 wt% in H2O, 99.99%).

Reaction streams were generated as-needed for each experiment. To generate the 1.25M 2,4-difluoronitrobenzene solution with biphenyl, approximately 198.86 g of 2,4-difluoronitrobenzene was combined with approximately 46.3 g biphenyl in a 1L volumetric flask and diluted with ethanol to achieve a total volume of 1L. To prepare the 3.5M morpholine solution with bibenzyl, approximately 304.85 g of morpholine was combined with approximately 72.9 g bibenzyl in a 1L volumetric flask. This mixture was diluted to 1L with ethanol as well. Solutions were sonicated as needed to dissolve all solids and allowed to

re-equilibrate prior to topping the solution up to the desired volume. To ensure the accuracy of off-line HPLC analyses, the reaction mixture was quenched in-line with a 3.5M trifluoroacetic acid (TFA) solution, immediately following passing through the FTIR flow cell. To prepare the TFA solution, approximately 399.08 g trifluoroacetic acid is added to a 1L volumetric flask and diluted to 1L with ethanol. All solutions were transferred to Wheaton bottles for use. Acetonitrile solvent (~1L) was added to a Wheaton bottle for use as-is.

Reactor Automation:

Complete automation of the flow reactor platform was enabled using LabVIEW (National Instruments, 2017 SPI Full Developer Suite), a state machine architecture from JKI (https://www.jki.net/), and OPC UA capabilities within the Mettler Toledo framework. The custom LabVIEW code integrates equipment control and real-time data processing and analysis to enable the automated optimization. Each subgroup of commands (e.g., equipment inputs/outputs, data recording and write-to-file, optimization regressions/termination criteria checks) are formatted into individual states within the case structure that are queued either by asynchronous loop triggers or user-events, typically triggered when a variable reaches a threshold value or a Boolean value changes throughout the algorithmic workflow. After starting the initial circular dynamic design of experiments, the reactor platform is fully automated through termination and no user input is requested. A depiction of the LabVIEW generated user interface and code are provided in **Figure S3**.

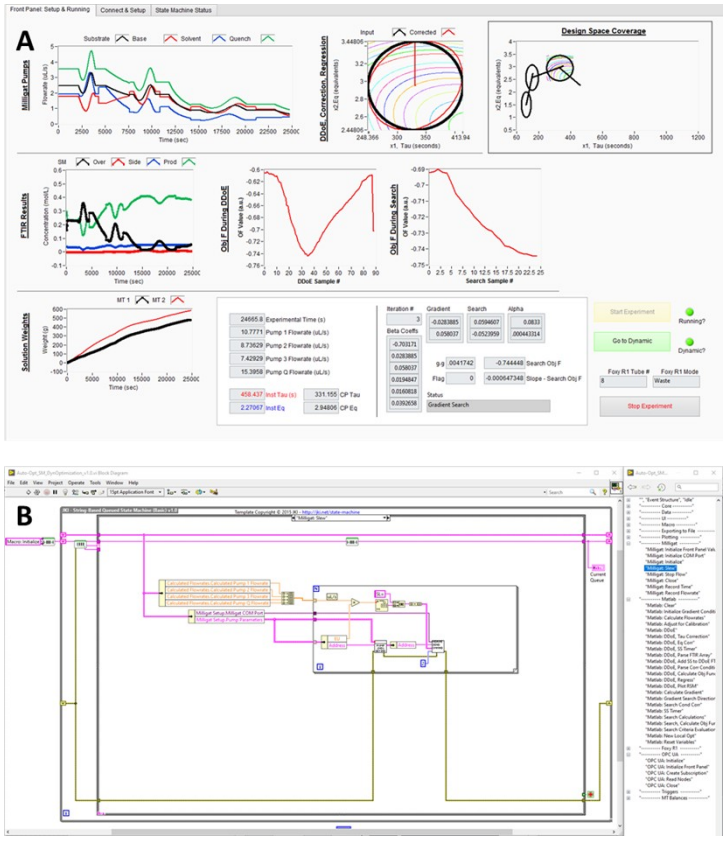

Figure S3. Illustration of the LabVIEW (A) user interface and (B) block diagram detailing the state machine architecture and command states

Correcting Reaction Conditions – Matlab:

Correction of conditions was performed using a custom Matlab code in which the time-dependent flowrate profile integrated over a variable time duration is compared to the measured reactor volume. Working backwards from the point of measurement, a minimizer is used to equate the calculated and measured reaction volume in order to calculate the associated initial and final reaction times, from which residence time and equivalents can be extracted. At a high level, the algorithm is based on the following:

$$\min\left[\left(V_{reactor+dead} - \int_{t_f}^{t_{meas}} Q_{reactor+dead}(t)dt\right)^2\right] \quad \text{(Eq. S2)}$$

$$\min\left[\left(V_{reactor} - \int_{t_i}^{t_f} Q_{reactor}(t)dt\right)^2\right] \quad \text{(Eq. S3)}$$

Knowing the flowrate profile, Eq. S2 is solved to calculate a final reaction time, t_f, for each measurement time, t_{meas}. Subsequently, Eq. S3 is then used to calculate the initial reaction time, t_i. With these variables calculated, characterization of the reaction conditions becomes facile.

Residence Time Distributions:

The ability to accurately correct/predict reaction conditions when a reactor is operated under dynamic flow mode is predicated on the reactor behaving as an ideal plug-flow reactor, exhibiting minimal axial dispersion throughout. The work presented herein leverages the same reactor as previously reported work [B.M. Wyvratt, J.P. McMullen and S.T. Grosser, *React. Chem. Eng.*, 2019, **4**, 1637-1645]. In that work, residence time distribution studies aimed at evaluating axial dispersion were performed; the raw data was fit to well-known dispersion models [O. Levenspiel. *Chemical Reaction Engineering*, John Wiley & Sons, Inc., New York, ed. 3, 1999] to obtain estimates on the dispersion number, D/uL, at 0.5- and 10-minute residence times. Both condition sets yielded dispersion numbers significantly less than 0.01, the threshold below which a reactor exhibits plug flow behavior per Levenspiel. Given that the exact same reactor (e.g., tubing, length) was leveraged for this work and similar conditions (0.5 to 10 min vs. 1 to 20 min residence times) were employed, additional residence time distribution studies were not required.

Penalty Function Definition:

As presented in the main text (Eq. 5), the objective function is defined by four key components, a productive term as well as three separate penalty terms. The productive term is simply the quantification of the yield of the desired product relative to the starting material concentration, defined as the concentration of 4-(5-fluoro-2-nitrophenyl)morpholine divided by the initial concentration of 2,4-difluoronitrobenzene at the point of mixing. The three penalty terms, P_1, P_2, and P_3, help to drive conditions towards an optimal solution satisfying reaction yield needs while controlling excessive double addition impurity growth, morpholine equivalent usage or long residence times. These terms are described as piecewise functions below in Eq. S4-S6.

$$P_1 = 0.1 * \left(\frac{100 \cdot [4]}{[1]_0} - 2\right)^2 \quad \begin{matrix} 0 & \frac{100 \cdot [4]}{[1]_0} \leq 2 \\ & 2 < \frac{100 \cdot [4]}{[1]_0} < 5.2 \\ 1 & \frac{100 \cdot [4]}{[1]_0} \geq 5.2 \end{matrix} \qquad \text{(Eq. S4)}$$

$$P_2 = \begin{cases} 0 & Equiv_{Morpholine} \leq 2 \\ 0.4 * \left(\frac{Equiv_{Morpholine}}{2} - 1\right)^2 & 2 \leq Equiv_{Morpholine} \leq 4 \end{cases} \qquad \text{(Eq. S5)}$$

$$P_3 = \begin{cases} 0 & \tau_{Reaction} \leq 10 \\ 0.4 * \left(\frac{\tau_{Reaction}}{10} - 1\right)^2 & 10 \leq \tau_{Reaction} \leq 20 \end{cases} \qquad \text{(Eq. S6)}$$

Dynamic Design of Experiments:

DOE designs

Numerous DOE designs amenable to dynamic conditions were considered and investigated through simulations. Figure S4 shows simulations of circular- and cardioid-based DOE designs under consistent conditions (5 minute residence time, 75 and 300 minute dynamic time). The instantaneous input conditions and corrected reaction conditions are shown in black and red lines, respectively. While the cardioid provides numerous benefits in the form of a balanced dataset across the design space, numerous reproducibility points at the center, and the ability to traverse the design *and* obtain centerpoint data without requiring a step change, the corrected conditions are quite convoluted due to the speed at which the system has to move through the design within the allotted dynamic time. Conversely, while the centerpoint requires a step change to obtain centerpoint data, the alignment between input and corrected conditions is significantly improved. Cardioid-based designs would require lengthy dynamic times (300+ minutes at τ = 5 min) to obtain acceptable agreement between input and corrected conditions. As such, a conscious choice was made to accept a required step change to obtain the centerpoint to enable a more rapid DOE, thereby reducing both experimental time but also resource/material burden.

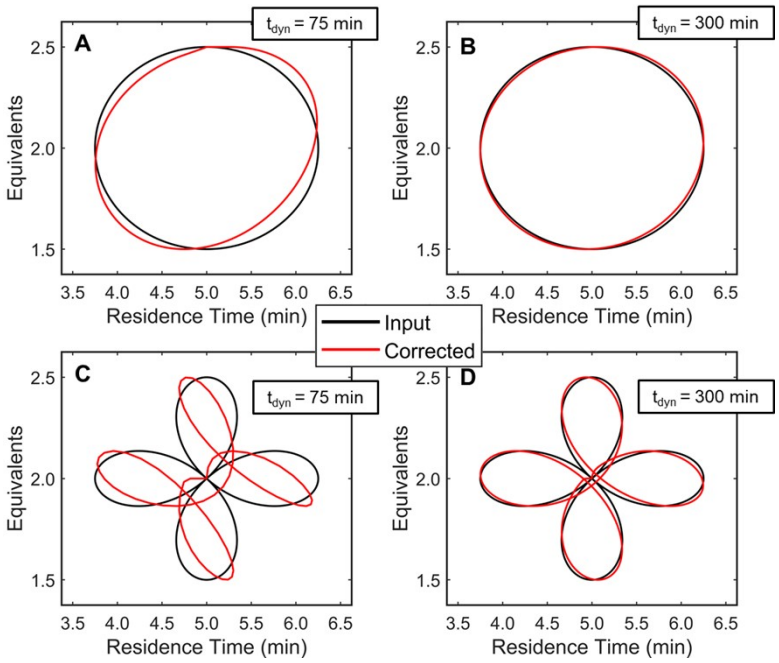

Figure S4. Comparison of circular (A,B) and cardioid (C,D) DOE designs from both an instantaneous input and corrected conditions perspective at differing dynamic times (75 or 300 minutes). The DOE centerpoint and variation for all simulations was [5 ± 1.25 min, 2.0 ± 0.5 equiv].

Simulations to optimize circular DOE input-corrected translatability

As highlighted previous in literature [2,3], due to the finite holdup volumes associated with the flow reactor itself, instantaneous changes made at the reactor inlet are not immediately realized at the outlet. As such, under dynamic or transient flow conditions, care must be taken to ensure that the conditions represent those actually experienced by a specific fluid element, corrected for any instantaneous changes in flowrate leveraging Equations (1-4) in the main text, included again below for convenience.

$$V_{Reactor} = \int_{t_i}^{t_f} Q(t)dt \qquad \text{(Eq. S7)}$$

$$\tau = t_f - t_i \qquad \text{(Eq. S8)}$$

$$V_d = \int_{t_f}^{t_{meas}} [Q(t) + Q_{quench}(t)]dt \qquad \text{(Eq. S9)}$$

$$Base\ Eq(t_{meas}) = \frac{C_{Base} Q_{Base}(t_i)}{C_{SM} Q_{SM}(t_i)} \qquad \text{(Eq. S10)}$$

An appropriate understanding of the deviation of the corrected conditions from those target conditions established by the instantaneous flowrates is critical to obtaining accurate, predictive response surface models intended to guide the optimization path. Ideally, "experiments" within the circular DOE would exhibit comparable weighting to all variables with minimal skew/bias in any one direction over others.

Recognizing the delay between setting conditions and realizing the change due to the finite holdup volumes, numerous simulations were performed in an attempt to standardize the dynamic DOE and resulting design space studied following correction of conditions. Results from a subset of the simulations are shown in Figure S5. On a high level, it is quite evident from the deviation of the corrected conditions from the instantaneous conditions that longer residence times (e.g., 15 min) coupled with shorter dynamic times (e.g., 30 min) lead to a poor decision space coverage. Admittedly, this is expected as the system is undergoing large input changes before fluid elements are able to make their way through the reactor at these longer residence times. Conversely, at a dynamic time of 300 min, the corrected conditions closely match the instantaneous input conditions, though a trend still exists showcasing better agreement for the shorter residence times than the longer residence times. Enlightening about this dataset though were the similarities in response identified for specific combinations of residence time and dynamic time. That is, the shape of design space coverage for the corrected conditions were identical for equivalent $t_{dynamic}/\tau_{reaction}$ ratios as seen in a few highlighted comparisons (red and blue boxes) within Figure S5. This relationship was leveraged to ensure that the circular dynamic DOE was consistent both within each experiment and from optimization run to run. A $t_{dynamic}/\tau_{reaction}$ ratio of 15 (simulations highlighted in red) was selected as an appropriate trade-off between DOE time requirements and minimal bias/data weighting concerns. In practice, the dynamic time is calculated for each DOE based on the residence time of the new DOE centerpoint and the response surface regression/analysis is universal to any centerpoint in the design space.

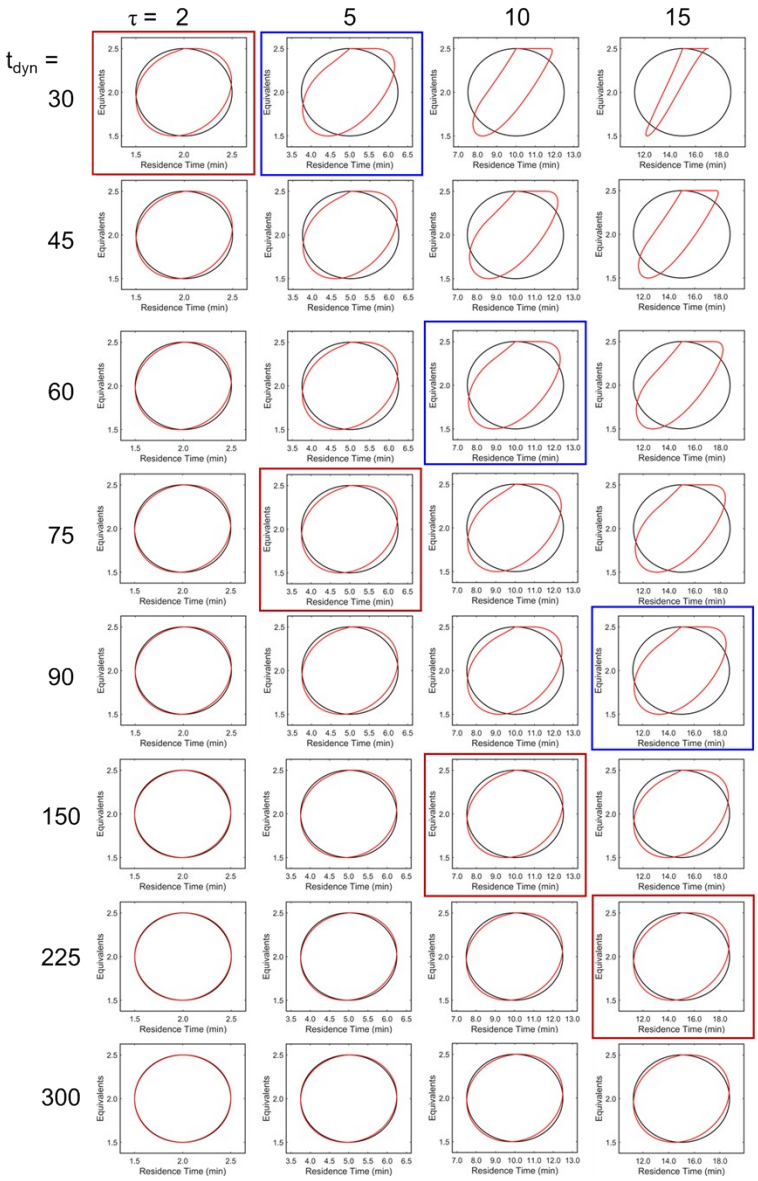

Figure S5. Simulations performed comparing the instantaneous input conditions to the corrected conditions from the circular dynamic DOE at various residence time and dynamic time conditions.

Experiment centered at [τ, Equiv]$_0$ = [2 min, 1.5 equiv]

As part of the holistic algorithm development, focused experiments were performed to evaluate the execution of a dynamic circular design of experiments and regression sequence within the LabVIEW code. A dynamic DOE, centered at [τ, Equiv]$_0$ = [2 min, 1.5 equiv], was performed with a total dynamic time of 30 minutes, consistent with a $t_{dynamic}/\tau_{reaction}$ ratio of 15 and the reaction performance analyzed via HPLC and FTIR. Concentration results from this experiment as a function of time on stream and design space conditions are presented in **Figure S6A** and **B**. FTIR and HPLC alignment was superb for all species. Trends in the conversion are clearly evident in **Figure S6B** with improved conversion occurring at higher morpholine equivalents and longer residence times, as expected. The concentration results and reaction conditions are together converted to a scalar objective function, shown in **Figure S6C** and **D**, which as expected, show excellent alignment between the FTIR and HPLC datasets. Within the sequential algorithm, the FTIR-based objective function reaction data was regressed against the reaction conditions (also corrected within the algorithm sequence), fitting to a quadratic function. The regression results are presented in figure (**Figure S7**) and tabulated form (**Table S3**). Overall, the model fit was excellent, exhibiting sum of squared errors (SSE), Akaike Information Criterion (AIC) and R-squared values of 0.0002567, -612.3, and 0.9994, respectively. In **Figure S7**, the raw data is presented against a contour mesh as predicted by the model fit from multiple views, highlighting a clear direction towards improved objective function values. Further, the contour plot resulting from the response surface regression along with a parity plot comparing the actual-to-predicted objective function values is provided in **Figure S8**. The model fit results are presented in **Table S3**, listing the model coefficients along with the calculated gradient and search vectors.

Results indicate that the algorithm responsible for the experimental design, results manipulation/transformation, and regression to generate a model performed adequately. Worth noting, **Figure S6**A shows excellent agreement between the HPLC and FTIR results, showcasing the predictive power of the PLS model trained by the one-dimensional data sets. This experimental dataset was leveraged in the "test" dataset shown in Figure S2. Additionally, **Figure S6**B and **Figure S6**D offer confidence in the accuracy of the response surface model generation process, indicating minimal error between the experimental data and values predicted by the obtained quadtratic model describing the space.

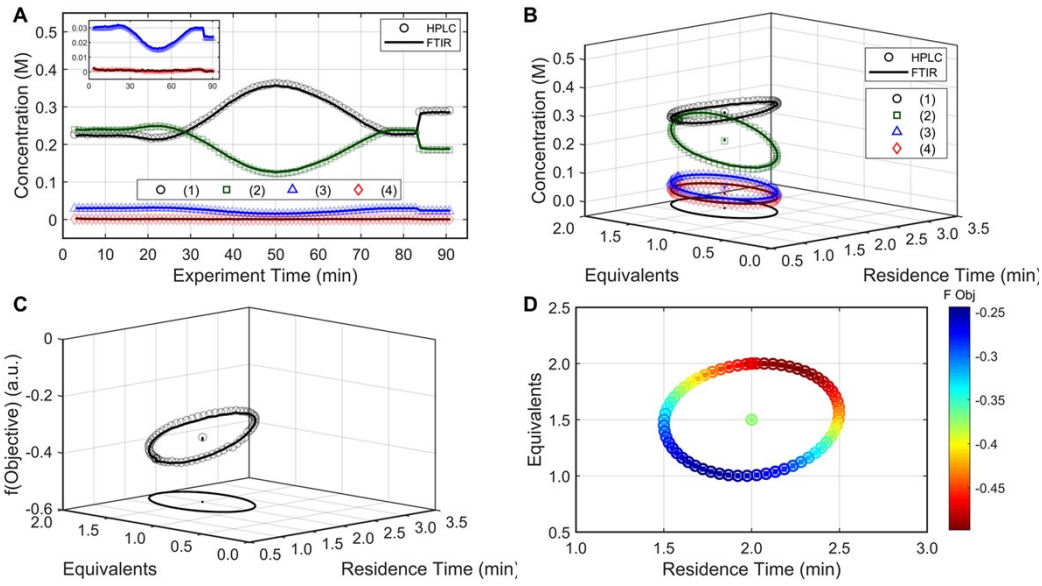

Figure S6. Results from the dynamic design of experiments centered around [2 min, 1.5 equiv]. (A) Concentration data presented as a function of time on stream for both the HPLC and FTIR analytical techniques for the species: (1) 2,4-difluoronitrobenzene, (2) 4-(5-fluoro-2-nitrophenyl)morpholine), (3) 4-(3-fluoro-4-nitrophenyl)morpholine), (4) 4,4'-(4-nitro-1,3-phenylene)dimorpholine. (B) Reaction concentration data as a function of the corrected reaction conditions, presented against the design space (x-y plane). (C,D) The resulting objective function values (from both HPLC [○,□,Δ,◊] and FTIR (-) datasets) plotted as a function of reaction conditions both in 3-dimensional and heatmap form.

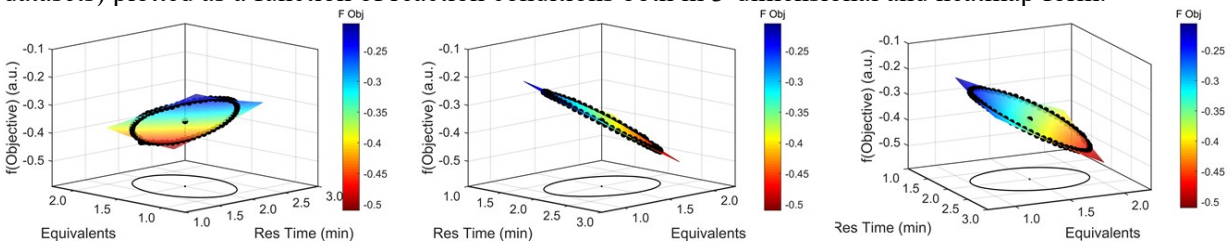

Figure S7. 3-dimensional plots of the objective function raw data plotted again the response surface model prediction in various views.

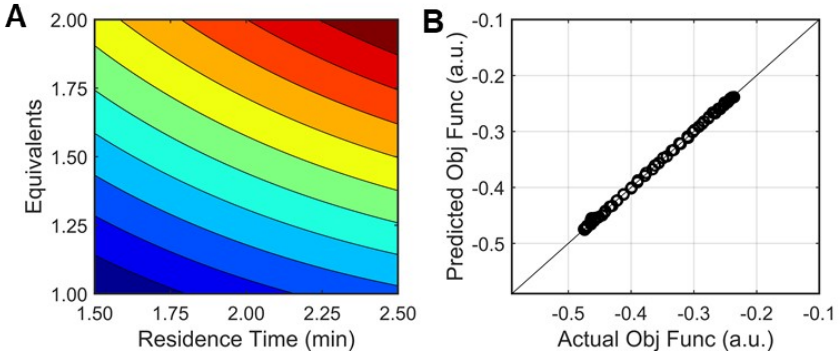

Figure S8. Results from the dynamic design of experiment centered at [x_1,x_2] = [2 min, 1.5 equiv]. (A) Contour plot of the response surface model obtained. (B) Parity plot of the experimental data against predicted objective function values based on the regressed model.

Table S3. Table summarizing the RSM results and calculated gradient/search vector obtained from the dynamic design of experiments starting at $[\tau, \text{Equiv}]_0 = [2 \text{ min}, 1.5]$.

Tau_{CP} (min)	Equiv_{CP}	β_0	β_1	β_2	β_{12}	β_{11}	β_{22}	$g(x_{Coded})$	$p(x_{Coded})$
2	1.5	-0.3565	-0.0496	-0.1025	-0.0117	0.0058	0.0044	[-0.0496, -0.1025]	[0.0496, 0.1025]

Experiment centered at $[\tau, Eq]_0 = [15 \text{ min}, 3.0 \text{ eq}]$

Similarly, a dynamic DOE, centered at $[\tau, \text{Equiv}]_0 = [15 \text{ min}, 3.0 \text{ eq}]$, was performed with the intent to understand the reaction performance under conditions more prone to overreaction in order to assess the impact of penalty functions on the resulting objective function values and response surface model directionality. The total dynamic time for this study was 225 minutes, again consistent with a $t_{dynamic}/\tau_{reaction}$ ratio of 15. Concentration results, shown in **Figure S9A** and **B**, convey the relative insensitivity of the desired product (green) levels to the reaction conditions in this design subspace. Instead, the overreaction impurity to 4,4'-(4-nitro-1,3-phenylene)dimorpholine (red) exhibits greater sensitivity, largely coupled to the side reaction levels. Given the weighty penalty on excessive levels of the overreaction impurity as expressed by Eq. S4 above, objective function values achieve elevated levels and appear to exhibit a discontinuity when compared against the design space, likely due to the discrete nature of the penalty function on the overreaction impurity. This stark change in experimental objective function values is evident in **Figure S9C** as well as the images in **Figure S10A**. Despite the discontinuity, the RSM fit to the experimental data is still quite reasonable as illustrated by parity plot (**Figure S10C**) as well as the SSE, AIC, and R^2 values from the regression (0.682, -779.1, 0.984, respectively). The gradient directionality and search direction from the resulting model fit appear appropriate for the dataset (**Figure S10B** and **Table S4**).

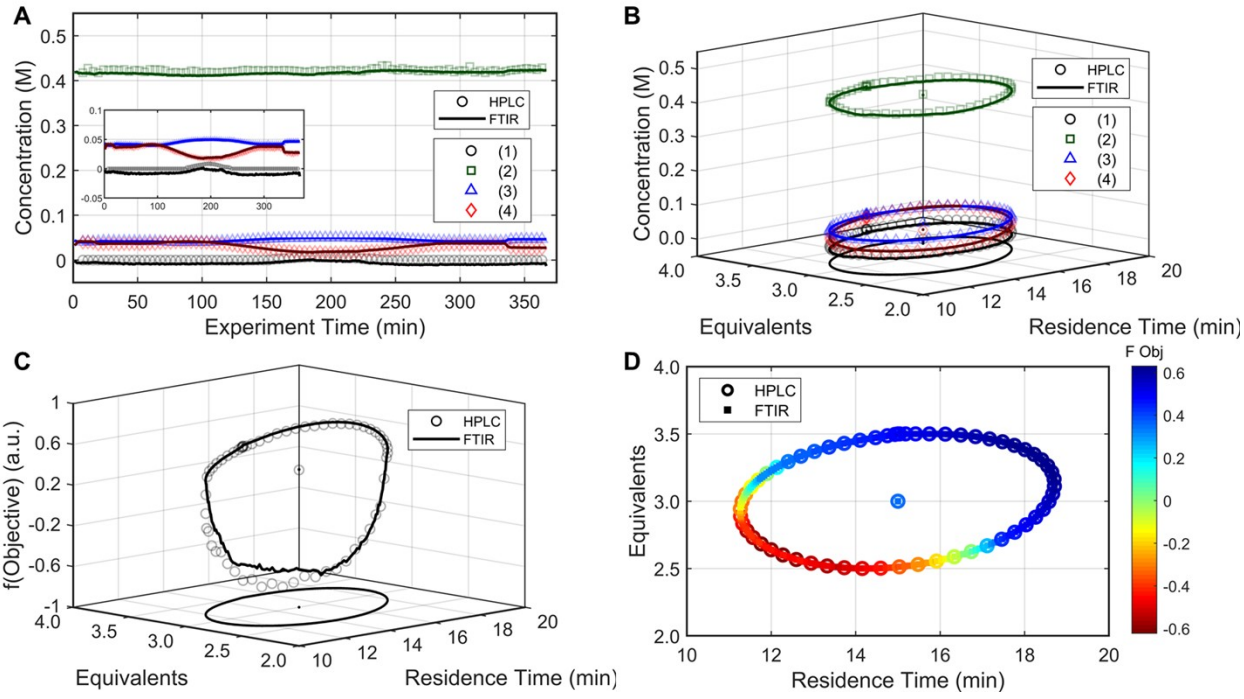

Figure S9. Results from the dynamic design of experiments centered around [15 min, 3.0 equiv]. (A) Concentration data presented as a function of time on stream for both the HPLC and FTIR analytical techniques for the species: (1) 2,4-difluoronitrobenzene, (2) 4-(5-fluoro-2-nitrophenyl)morpholine), (3) 4-

(3-fluoro-4-nitrophenyl)morpholine), (4) 4,4'-(4-nitro-1,3-phenylene)dimorpholine. (B) Reaction concentration data as a function of the corrected reaction conditions, presented against the design space (x-y plane). (C,D) The resulting objective function values (from both HPLC [○] and FTIR (-) datasets) plotted as a function of reaction conditions both in 3-dimensional and heatmap form.

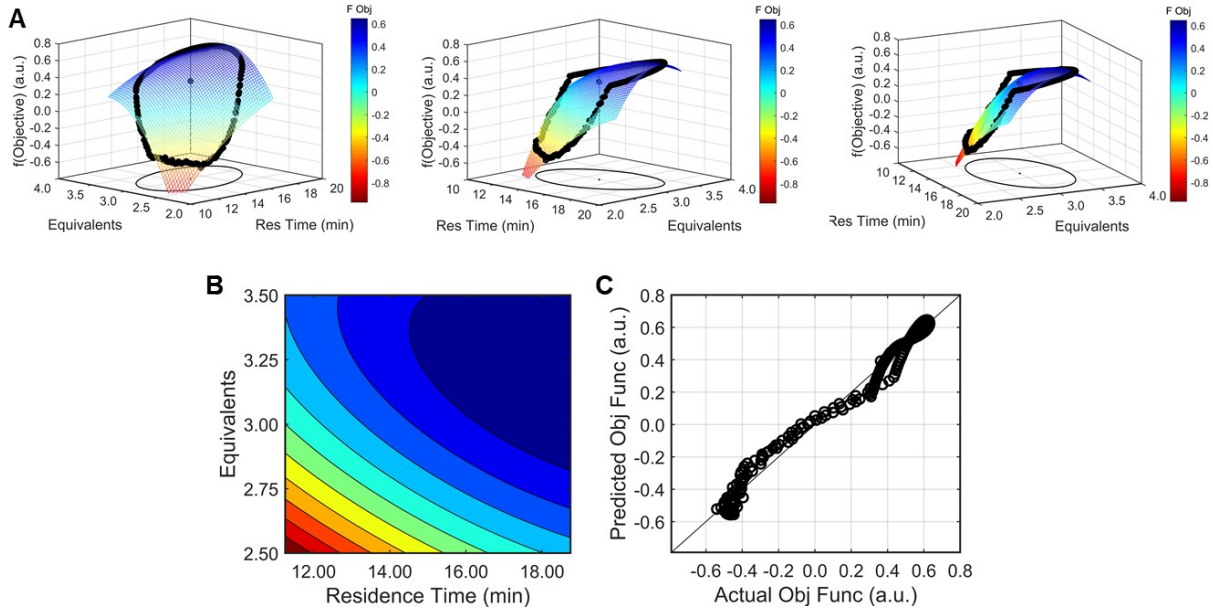

Figure S10. (A) 3-dimensional plots of the objective function raw data plotted again the response surface model prediction in various views from the dynamic design of experiments starting at $[\tau, \text{Equiv}]_0 = [15 \text{ min}, 3.0]$. (B) Contour plot of the RSM over the design space. (C) Parity plot of the predicted objective function generated via the RSM against the actual objective function.

Table S4. Table summarizing the RSM results and calculated gradient/search vector obtained from the dynamic design of experiments starting at $[\tau, \text{Equiv}]_0 = [15 \text{ min}, 3.0]$.

Tau_{CP} (min)	Equiv_{CP}	β_0	β_1	β_2	β_{12}	β_{11}	β_{22}	$\mathbf{g(x_{Coded})}$	$\mathbf{p(x_{Coded})}$
15	3.0	0.3920	0.3496	0.3985	-0.1939	-0.1312	-0.2895	[0.3496, 0.3985]	[-0.3496, -0.3985]

Automated Optimization Runs:

Optimization Experiment Starting at $[\tau, Eq]_0 = [2 \text{ min}, 1.5 \text{ eq}]$

See main text for the bulk of results from the optimization run starting at [2 min, 2.0 eq]. That said, Table S5 provides greater details into the response surface model, gradient and search directions.

Table S5. Table summarizing the series of RSMs and calculated gradient/search vectors obtained during the progression through the automated optimization run starting at $[\tau, \text{Equiv}]_0 = [15 \text{ min}, 3.5]$.

RSM #	1	2	3	4	5
Tau_{CP} (min)	2.0	2.62	5.52	7.61	10.23
Equiv_{CP}	1.5	2.577	2.948	2.381	2.372
β_0	-0.361	-0.591	-0.703	-0.740	-0.769
β_1	-0.054	-0.077	-0.028	-0.029	-0.001
β_2	-0.098	-0.004	0.058	-0.024	-0.004
β_{12}	-0.005	0.010	0.020	0.013	0.033
β_{11}	0.000	0.017	0.016	0.006	0.027
β_{22}	0.000	0.030	0.039	0.044	0.061
$g(x_{Coded})$	[-0.054, -0.098]	[-0.077, -0.0043]	[-0.028, 0.058]	[-0.029, -0.024]	[-0.001, -0.004]
$p(x_{Coded})$	[0.054, 0.098]	[0.083, 0.015]	[0.060, -0.052]	[0.057, -0.001]	- [#]
g•g	0.0125	0.0060	0.0042	0.0014	2×10^{-5}

[#] Algorithm terminated due to optimum internal to RSM as confirmed by the Hessian of the RSM.

Optimization Experiment Starting at $[\tau, \text{Equiv}]_0 = [15 \text{ min}, 3.5 \text{ equiv}]$

To evaluate the reproducibility of an discovered optimal result and ensure that a local optima was not discovered, the optimization was also performed from a different starting point, [15 min, 3.5 equiv]. The experiment consisted of one search sequence and 3 total design of experiments with the discovered optimum located within the final DOE as shown by the Hessian of the RSM. **Figure S11** provides details into the reaction conditions employed (Figures A-C) as well as the concentration and objective function results (D, E) as a function of time on stream. Corrected conditions again matched very closely to the instantaneous input conditions, owing to appropriate choices for the dynamic times for the search and DOE operations. Overall, the optimization progresses rapidly from an area with excessive penalization due to elevated overreaction levels and high residence time/equivalents values to an area very close to the optimum showing a decrease in objective function from ~0.5 to -0.6 after a single search (see **Figure S11E** and **Figure S12**). There is a clear discontinuity in the search data results, owing to the discrete changes in the overreaction penalty function as illustrated in Eq. S4. Response surface model results are shown in **Figure S13** in various forms: (top row) experimental objective function results superimposed against a contour mesh generated from the RSM prediction, (middle row) 2-dimensional contour plots showing the directionality of the objective function values across the design space studied in each design of experiments, (bottom row) parity plot comparing the actual objective function values to those predicted by the RSM. Additional "views" of the top row of plots are provided in **Figure S14** to better illustrate the curvature and model fit for the various DOEs/RSMs. There are two key aspects to note from **Figure S13** and **Figure S14**. First, It is quite evident from the curvature associated with each subsequent RSM and the associated contour plot that the system progresses from an area characterized by a steep gradient to one consisting with concavity and a minimum value. RSM #2 predicted an optimum in the lower right quadrant of the design subspace (~10 min, 2.23 equiv) and the subsequent circular dynamic DOE centered at this predicted optimum confirmed the result (terminating with a predicted optimum of 10.0 min, 2.26 equiv). The second point to be made from these results stems from the stark differences in response surface model accuracy between the optimization experiment initiated at [2 min, 2.0 equiv] and that initiated at [15 min, 3.5 equiv]. The model fits exhibit a significantly lower sum of squared error for most of the RSMs from the

optimization from [2 min, 2.0 equiv] as seen in Figure 11 of the main text relative to those in [15 min, 3.5 equiv] (see **Figure S13**). While this is potentially due to experimental error associated with the FTIR data, it is more likely due to the larger implementation of penalty functions in these areas of interest that generate some discontinuities/atypical curvature in the responses. Response surface model results are summarized in **Table S6** as well.

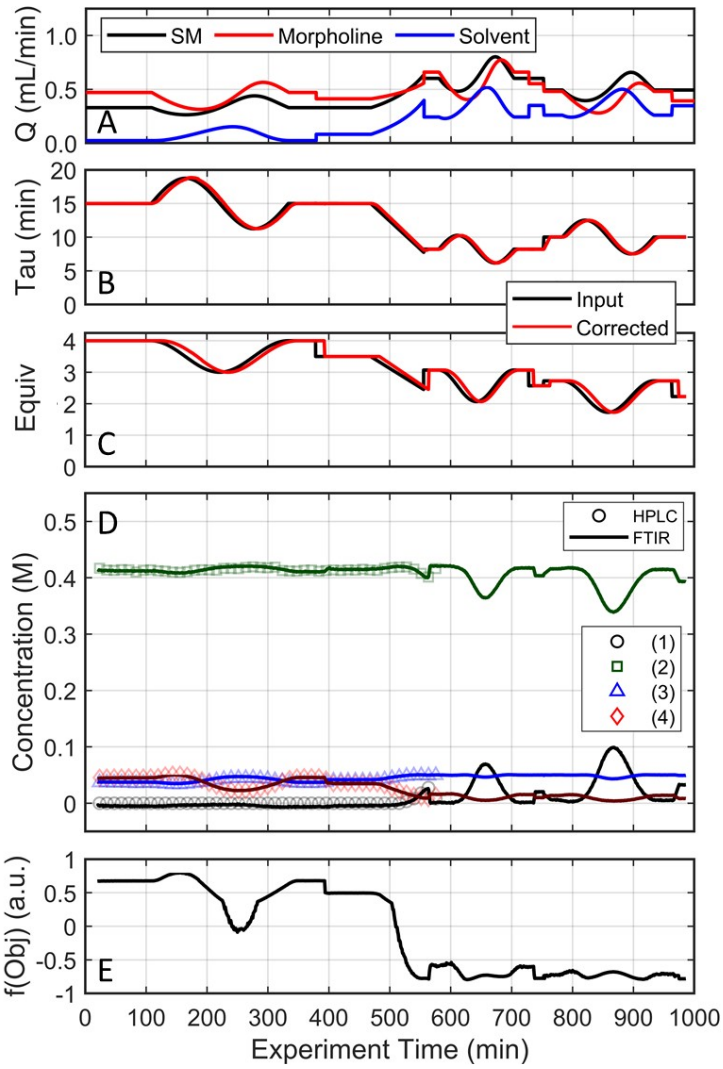

Figure S11. Conditions and experimental results from the automated optimization run starting from [15 min, 3.5 equiv] presented as a function of experimental time on stream. (A) Flowrates for the 3 streams combined to drive the reaction and control conditions: 2,4-difluoronitrobenzene (SM), Morpholine (Base) and Ethanol (Solvent). (B,C) Instantaneous/input conditions and subsequently corrected conditions as a function of time on stream. (D) HPLC and FTIR data results for the 4 species: (1) 2,4-difluoronitrobenzene, (2) 4-(5-fluoro-2-nitrophenyl)morpholine), (3) 4-(3-fluoro-4-nitrophenyl)morpholine), (4) 4,4'-(4-nitro-1,3-phenylene)dimorpholine. (E) Calculated objective function based on the FTIR results and corrected conditions as a function of experiment time.

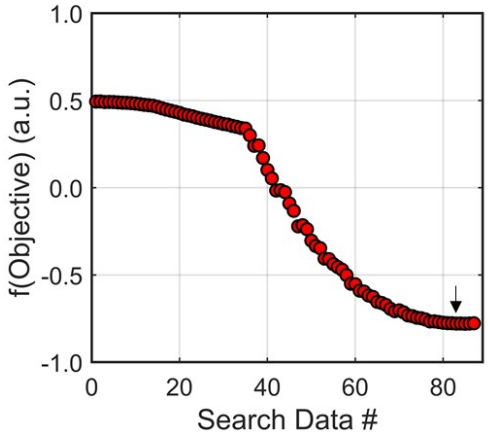

Figure S12. Search progression results for the first (and only) search in the optimization experiment starting at $[\tau, \text{Equiv}]_0$ = [15 min, 3.5 equiv]

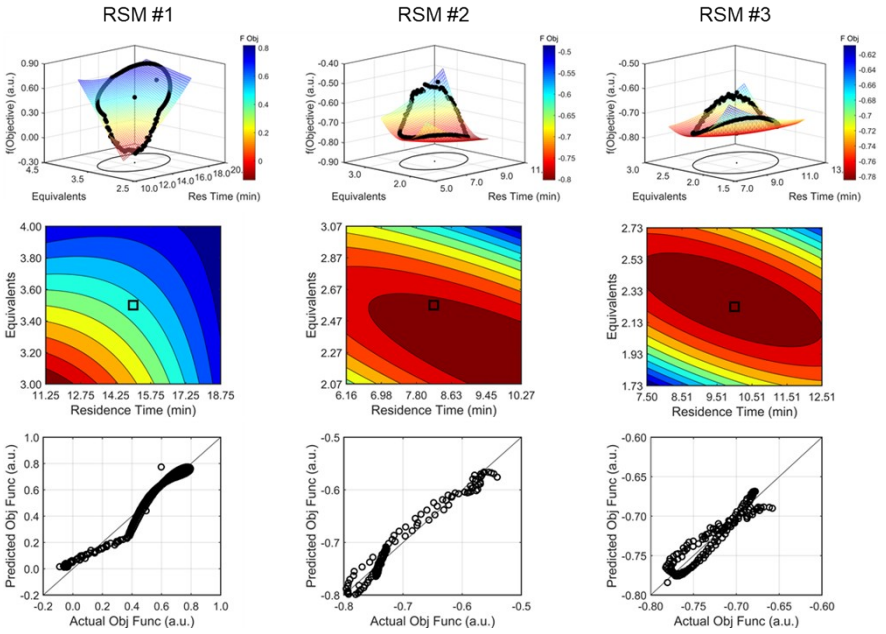

Figure S13. Response surface model results for the various DOEs performed during the automated optimization run starting from [15 min, 3.5 eq]. Each DOE and regression is represented within each column. (Top Row) Comparison of the experimental objective function results and the response surface model mesh against the design space region. (Middle Row) Contour plot describing the response surface model and directionality. (Bottom Row) Parity plots of the experimental data against the predicted values based on the RSM.

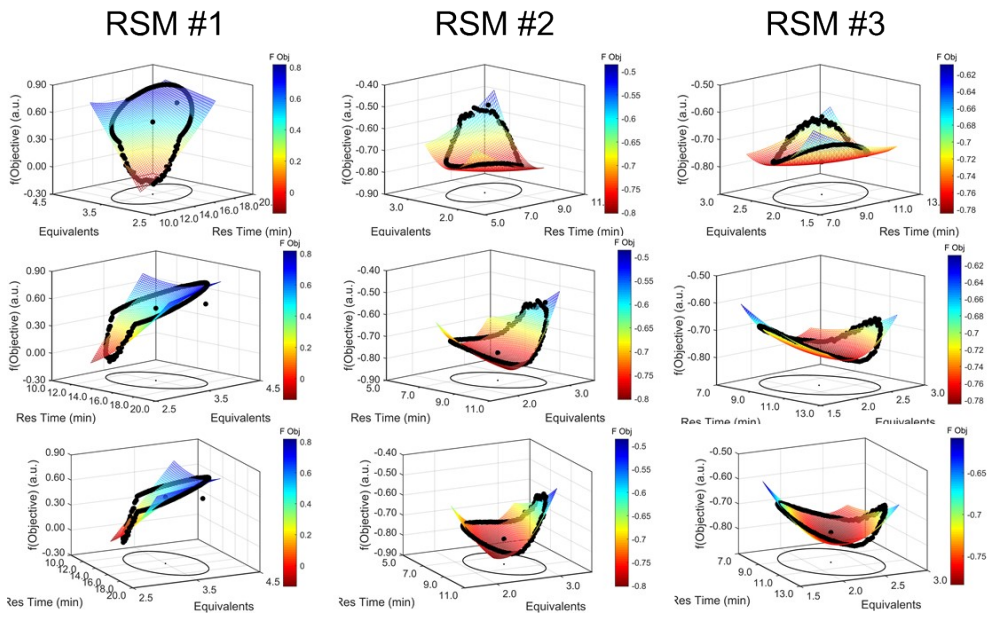

Figure S14. Various views showing the comparison of the experimental objective function results and the response surface model mesh against the design space region for the automated optimization run starting from [15 min, 3.5 equiv]. Different views of the data are provided in the various rows for a given RSM.

Table S6. Table summarizing the series of RSMs and calculated gradient/search vectors obtained during the progression through the automated optimization run starting at $[\tau, \text{Equiv}]_0 = [15 \text{ min}, 3.5]$.

RSM #	1	2	3
Tau_{CP} (min)	15.00	8.22	10.00
Equiv_{CP}	3.50	2.57	2.23
β_0	0.4410	-0.7816	-0.7841
β_1	0.2283	0.0090	-0.0026
β_2	0.2475	0.0706	-0.0110
β_{12}	-0.1877	0.0838	0.0581
β_{11}	0.0882	0.0276	0.0249
β_{22}	0.0000	0.1052	0.0791
$g(x_{Coded})$	[0.2283, 0.2475]	[0.0090, 0.0706]	[-0.0026, -0.0110]
$p(x_{Coded})$	[-0.2283, -0.2475]	[0.0201, -0.0390]	- [#]
g•g	0.1134	0.0051	0.00013

[#] Algorithm terminated due to optimum internal to RSM as confirmed by the Hessian of the RSM.

Comparing Optimization Run results to Steady State Results

A separate experiment was performed following the two automated optimization experiments in an effort to evaluate the accuracy of the autonomous system relative to traditional steady state experiments. In that experiment, reactions were performed under steady state at the two optimum conditions as determined by the algorithm. Overall, the automated optimization and steady state results algin well.

Table S7. Comparison of the results at or near the determined optimum obtained either during the automated optimization experiment or subsequent, confirmatory steady state experiments.

	Conditions				Concentration (M)				
	Tau (min)	Equiv	Method	Analytical	2,4-difluoronitrobenzene	4-(5-fluoro-2-nitrophenyl)morpholine	4-(3-fluoro-4-nitrophenyl)morpholine	4,4'-(4-nitro-1,3-phenylene)dimorpholine	Fobj
Optimization Run #1	10.2	2.37	Auto-Opt	FTIR	0.04263	0.39042	0.05074	0.00599	-0.767
				HPLC	0.02590	0.38930	0.04414	0.00892	-0.765
	10.2	2.39	Steady State	FTIR	0.03125 ± 0.00063	0.39450 ± 0.00039	0.05071 ± 0.00007	0.00727 ± 0.00019	-0.774
				HPLC	0.02334 ± 0.00071	0.39757 ± 0.00165	0.05088 ± 0.00047	0.01026 ± 0.00007	-0.779
Optimization Run #2	10.0	2.2269	Auto-Opt	FTIR	0.0331	0.39275	0.04957	0.00841	-0.780
				HPLC	-	-	-	-	-
	10.0	2.26	Steady State	FTIR	0.04118 ± 0.00060	0.38581 ± 0.00011	0.05004 ± 0.00000	0.00604 ± 0.00019	-0.765
				HPLC	0.03374 ± 0.00101	0.39152 ± 0.00153	0.04946 ± 0.00194	0.00874 ± 0.00018	-0.776

Comparison of response surface model structure on fits and predictions

As is typical practice for response surface modelling, a quadratic function was leveraged for describing the various RSMs generated during the optimization runs. That said, as part of platform development/validation and refinement, the dynamic design of experiments data results from the optimization run starting at [15 min, 3.5 equiv] were fit to linear, quadratic, and cubic functions (detailed in **Table S8**) in Matlab using the *stepwiselm* function post-run to validate the regression model selection; the predicted values based on the model fit were compared to the raw data for the various RSMs, both as a parity plot and by superimposing the raw data against a contour mesh of the regressed model. To summarize the datasets, as expected, the linear fits inadequately describe the response surface given the inability to fit an inherently convoluted, curved response surface associated with reaction kinetics and the applied penalty functions. While the cubic function provides the best model fit based on the parity plots, the models appear to be overfit, exhibiting features with little physical meaning, that can ultimately skew the gradient values used to inform the next search. Given this data, the use of quadratic functions to describe the RSMs in these optimization experiments is considered justified.

Table S8. Response surface model structures considered for regression against the circular dynamic DOE data

Model Type	**Function Structure**
Linear	$F(x) = \beta_0 + \beta_1 x_1 + \beta_2 x_2$
Quadratic	$F(x) = \beta_0 + \beta_1 x_1 + \beta_2 x_2 + \beta_{12} x_1 x_2 + \beta_{11} x_1^2 + \beta_{22} x_2^2$
Cubic	$F(x) = \beta_0 + \beta_1 x_1 + \beta_2 x_2 + \beta_{12} x_1 x_2 + \beta_{11} x_1^2 + \beta_{22} x_2^2 + \beta_{111} x_1^3 + \beta_{112} x_1^2 x_2 + \beta_{122} x_1 x_2^2 + \beta_2$

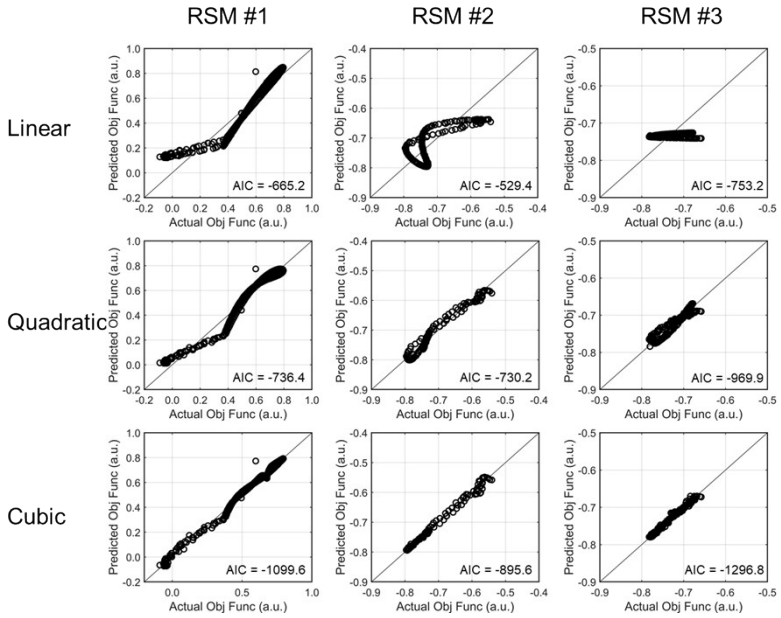

Figure S15. Parity plots of the experimental versus predicted objective function values for the three RSMs from the optimization run starting at [15 min, 3.5 equiv], but regressed using different functions

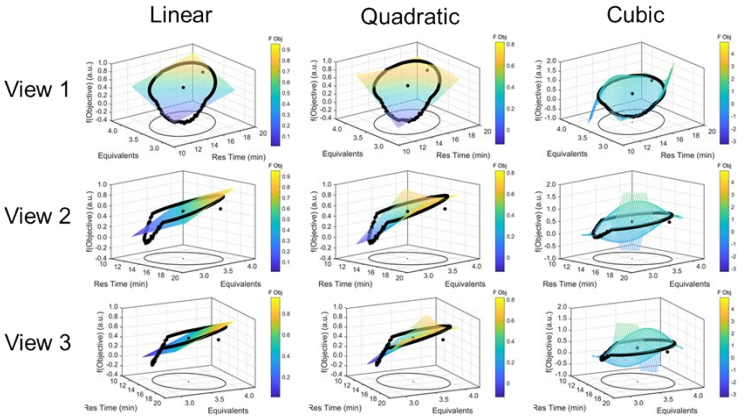

Figure S16. Experimental objective function results versus RSMs regressed to different functions for the **first** DOE/RSM from the optimization run starting at [15 min, 3.5 equiv]. Objective function improves from yellow to blue.

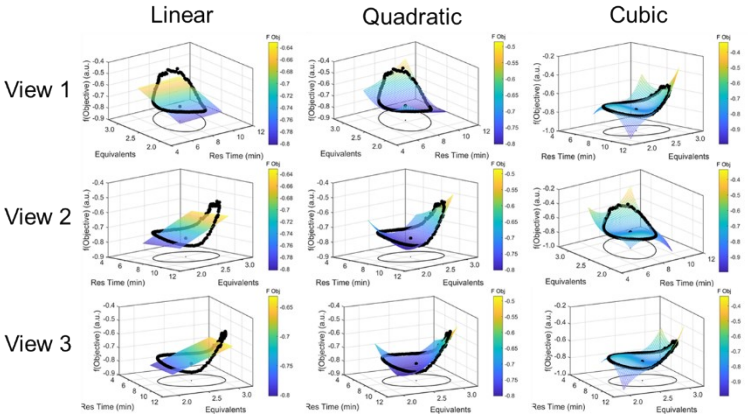

Figure S17. Experimental objective function results versus RSMs regressed to different functions for the **second** DOE/RSM from the optimization run starting at [15 min, 3.5 equiv]. Objective function improves from yellow to blue.

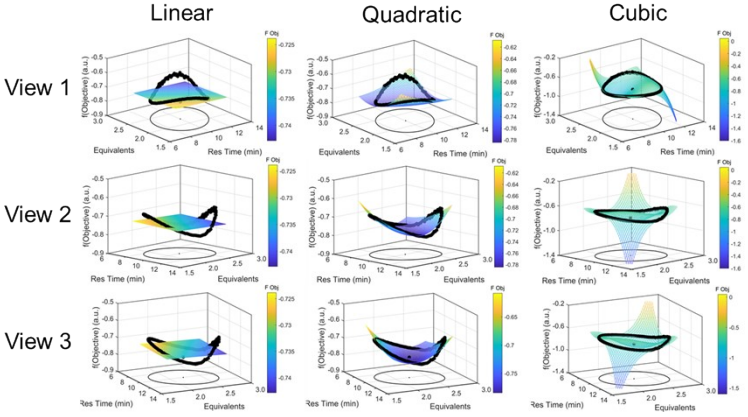

Figure S18. Experimental objective function results versus RSMs regressed to different functions for the **third (final)** DOE/RSM from the optimization run starting at [15 min, 3.5 equiv]. Objective function improves from yellow to blue.

Kinetic Modeling:

Kinetic modeling and parameter regression were performed in Matlab 2012b (Mathworks®). The reaction network given in Scheme S1 was described by the reaction rates and differential equations given .

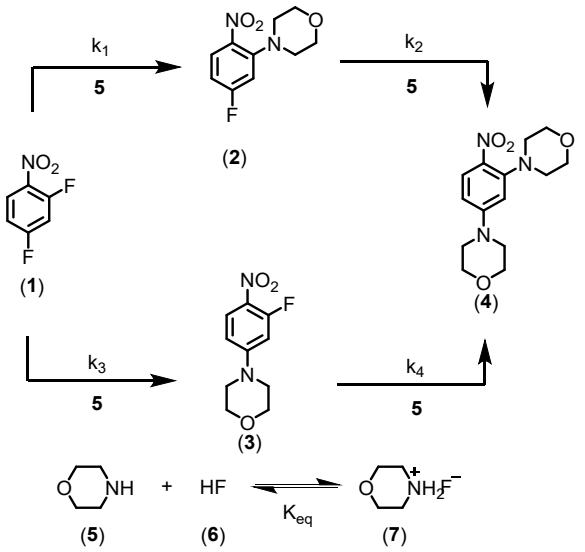

Scheme S1: Reaction network for case study S_NAr.

$$r_1 = -k_1[1][5] \qquad r_2 = -k_2[2][5]$$

$$r_3 = -k_3[1][5] \qquad r_4 = -k_4[3][5]$$

$$r_5 = -k_5\left([6][5] - \frac{1}{K_{eq}}[7]\right)$$

$$\frac{d[1]}{dt} = r_1 + r_3 \qquad \frac{d[2]}{dt} = -r_1 + r_2$$

$$\frac{d[3]}{dt} = -r_1 + r_4$$

$$\frac{d[4]}{dt} = -r_3 - r_4$$

$$\frac{d[5]}{dt} = r_1 + r_2 + r_3 + r_4 + r_5$$

$$\frac{d[6]}{dt} = -r_1 - r_2 - r_3 - r_4 - r_5$$

$$\frac{d[7]}{dt} = -r_5$$

Figure S19: Reaction rate expression and differential equations used in the kinetic modeling of S_NAr case study.

For a given set of corrected experimental conditions (residence time and initial morpholine equivalents), the solution to the network of differential equations was calculated using the Matlab function ode15s. The modeled concentration compounds **1**, **2**, **3**, and **4** were compared to corresponding FTIR concentration data from both dynamic optimization investigations. At points in the dynamic experiments, negative FTIR concentrations were observed and attributed to spectroscopic noise associated with the limit of detection of the FTIR or the resolution of the FTIR PLS model at low concentrations. To maintain physical constraints, these negative values were converted to "0" for the parameter regression. The acid-base neutralization reaction rate was considered rapid and the associated rate constant (k_5) was arbitrarily selected to be 10 $M^{-1}min^{-1}$. The equilibrium constant, Keq, was estimated from the pKa values for morpholine (pKa = 8.36) and HF (pKa = 3.8). These parameters remained fixed during regression. The Matlab function lsqnonlin was used to fit the rate constants k_1-k_4 to minimize the weighted sum of squared error term given in .

$$wSSE = \sum_{c=1}^{C}\sum_{i=1}^{N}\frac{\left(y_{i,c} - \hat{y}_{i,c}\right)^2}{max\left(y_c\right)} \qquad \text{(Eq. S11)}$$

Where $y_{i,c}$ is the FTIR concentration for species c (C is total number of species used in regression, 4) measured at corrected conditions for experiment i (N is total number of dynamic experiments, 1389), and $\hat{y}_{ic}$ is the model predictions for compound c for experiment i.

Optimization Experiment Data in Tabulated Format:

Optimization Run #1

Table S9. Tabulated data from the first optimization run starting at $[\tau, \text{Equiv}]_0 = [2 \text{ min}, 1.5]$

Tau (min)	Eq (-)	Obj Func (-)
2.003	2.000	-0.465
2.045	2.000	-0.466
2.130	1.999	-0.473
2.222	1.986	-0.480
2.306	1.955	-0.483
2.378	1.906	-0.481
2.434	1.841	-0.476
2.473	1.761	-0.465
2.493	1.669	-0.449
2.490	1.567	-0.429
2.466	1.460	-0.404
2.420	1.353	-0.377
2.355	1.251	-0.349
2.272	1.160	-0.321
2.175	1.085	-0.296
2.069	1.032	-0.274
1.960	1.004	-0.257
1.853	1.003	-0.248
1.753	1.028	-0.243
1.665	1.077	-0.245
1.594	1.147	-0.251
1.542	1.233	-0.263
1.511	1.329	-0.277
1.502	1.432	-0.295
1.515	1.535	-0.313
1.548	1.634	-0.335
1.600	1.727	-0.358
1.667	1.809	-0.381
1.748	1.878	-0.404
1.838	1.933	-0.425
1.931	1.973	-0.445
1.989	1.995	-0.459
2.000	1.500	-0.364
2.009	1.500	-0.363
2.025	1.514	-0.364
2.041	1.544	-0.363
2.057	1.573	-0.368
2.074	1.603	-0.376
2.090	1.632	-0.384
2.107	1.662	-0.390
2.123	1.691	-0.397
2.140	1.721	-0.407
2.156	1.750	-0.414
2.172	1.780	-0.421
2.189	1.809	-0.429
2.205	1.839	-0.437
2.222	1.868	-0.444
2.238	1.898	-0.452
2.255	1.927	-0.460
2.271	1.957	-0.467
2.287	1.986	-0.474
2.304	2.016	-0.480
2.320	2.045	-0.489
2.337	2.075	-0.496
2.353	2.104	-0.502
2.370	2.134	-0.508
2.386	2.163	-0.516
2.402	2.193	-0.520
2.419	2.222	-0.527
2.435	2.252	-0.531
2.452	2.281	-0.537
2.468	2.311	-0.542
2.484	2.340	-0.547
2.501	2.370	-0.552
2.517	2.399	-0.556
2.534	2.429	-0.560
2.550	2.458	-0.564
2.567	2.488	-0.564
2.583	2.518	-0.567
2.599	2.547	-0.561
2.616	2.577	-0.577
2.632	2.606	-0.575
2.649	2.636	-0.575
2.665	2.665	-0.575
2.682	2.695	-0.576
2.624	3.077	-0.580
2.668	3.077	-0.578
2.745	3.077	-0.579
2.840	3.072	-0.583
2.930	3.058	-0.591
3.013	3.033	-0.601
3.087	2.997	-0.610
3.150	2.952	-0.621
3.200	2.898	-0.632
3.236	2.835	-0.639
3.257	2.765	-0.646
3.262	2.689	-0.650
3.250	2.609	-0.651
3.221	2.527	-0.650
3.176	2.445	-0.646
3.116	2.365	-0.638
3.041	2.291	-0.625
2.954	2.224	-0.612
2.856	2.167	-0.595
2.752	2.123	-0.578
2.644	2.093	-0.561
2.534	2.078	-0.546
2.427	2.079	-0.531
2.326	2.095	-0.517
2.233	2.126	-0.509
2.151	2.170	-0.502
2.082	2.225	-0.496
2.028	2.290	-0.493
1.991	2.362	-0.491
1.969	2.438	-0.493
1.965	2.517	-0.494
1.977	2.596	-0.498
2.005	2.673	-0.503
2.048	2.747	-0.509
2.104	2.816	-0.519
2.172	2.878	-0.527
2.250	2.934	-0.534
2.336	2.981	-0.541
2.429	3.019	-0.551
2.522	3.048	-0.559
2.587	3.068	-0.565
2.616	2.577	-0.591
2.658	2.577	-0.600
2.722	2.577	-0.606
2.802	2.586	-0.607
2.882	2.597	-0.607
2.962	2.608	-0.612
3.042	2.618	-0.617
3.122	2.629	-0.623
3.201	2.640	-0.629
3.281	2.650	-0.634
3.361	2.661	-0.639
3.441	2.671	-0.641
3.521	2.682	-0.645
3.601	2.693	-0.649
3.681	2.703	-0.657
3.761	2.714	-0.660
3.841	2.725	-0.661
3.921	2.735	-0.666
4.001	2.746	-0.669
4.081	2.757	-0.671
4.161	2.767	-0.673
4.240	2.778	-0.677
4.320	2.788	-0.678
4.400	2.799	-0.679
4.480	2.810	-0.681
4.560	2.820	-0.684
4.640	2.831	-0.684
4.720	2.842	-0.686
4.800	2.852	-0.687
4.880	2.863	-0.687
4.960	2.874	-0.689
5.040	2.884	-0.689
5.120	2.895	-0.690
5.200	2.906	-0.691
5.279	2.916	-0.692
5.359	2.927	-0.694
5.439	2.937	-0.693
5.519	2.948	-0.695
5.599	2.959	-0.694
5.679	2.969	-0.693
5.527	3.448	-0.605
5.554	3.448	-0.605
5.597	3.448	-0.603
5.658	3.448	-0.606
5.734	3.448	-0.607
5.825	3.448	-0.606
5.920	3.447	-0.608
6.013	3.443	-0.608
6.104	3.437	-0.610
6.192	3.428	-0.611
6.277	3.417	-0.610
6.358	3.404	-0.617
6.434	3.389	-0.620
6.506	3.371	-0.621
6.572	3.351	-0.628
6.633	3.329	-0.635
6.688	3.305	-0.642
6.737	3.278	-0.647
6.780	3.250	-0.659
6.815	3.220	-0.661
6.843	3.189	-0.672
6.864	3.155	-0.682
6.878	3.121	-0.688
6.883	3.085	-0.694
6.881	3.048	-0.700
6.871	3.010	-0.707
6.853	2.972	-0.713
6.826	2.933	-0.719
6.792	2.894	-0.724

6.750	2.855	-0.728	6.250	2.797	-0.719	8.906	2.114	-0.735
6.701	2.816	-0.732	6.330	2.772	-0.722	8.826	2.089	-0.732
6.644	2.778	-0.734	6.410	2.748	-0.725	8.741	2.065	-0.726
6.580	2.740	-0.737	6.490	2.723	-0.727	8.653	2.043	-0.721
6.509	2.704	-0.741	6.570	2.699	-0.729	8.561	2.021	-0.717
6.432	2.669	-0.741	6.650	2.674	-0.732	8.466	2.001	-0.712
6.349	2.636	-0.745	6.730	2.650	-0.734	8.367	1.982	-0.707
6.261	2.605	-0.742	6.810	2.625	-0.738	8.266	1.964	-0.701
6.167	2.576	-0.740	6.890	2.601	-0.739	8.163	1.948	-0.696
6.069	2.549	-0.739	6.969	2.576	-0.740	8.058	1.934	-0.691
5.968	2.526	-0.736	7.049	2.552	-0.742	7.951	1.921	-0.689
5.864	2.505	-0.733	7.129	2.527	-0.743	7.843	1.910	-0.681
5.757	2.487	-0.729	7.209	2.503	-0.743	7.734	1.900	-0.679
5.648	2.472	-0.725	7.289	2.479	-0.744	7.624	1.893	-0.674
5.539	2.461	-0.722	7.369	2.454	-0.744	7.515	1.887	-0.671
5.430	2.453	-0.719	7.449	2.430	-0.745	7.406	1.883	-0.668
5.321	2.449	-0.715	7.529	2.405	-0.745	7.297	1.881	-0.665
5.213	2.448	-0.711	7.609	2.381	-0.747	7.190	1.881	-0.662
5.107	2.451	-0.705	7.689	2.356	-0.746	7.084	1.882	-0.660
5.005	2.457	-0.703	7.769	2.332	-0.747	6.980	1.886	-0.660
4.905	2.467	-0.699	7.849	2.307	-0.746	6.878	1.891	-0.658
4.810	2.480	-0.697	7.929	2.283	-0.744	6.778	1.898	-0.657
4.719	2.496	-0.693	7.609	2.881	-0.722	6.682	1.907	-0.656
4.633	2.515	-0.690	7.612	2.881	-0.722	6.588	1.917	-0.658
4.553	2.537	-0.687	7.628	2.881	-0.722	6.498	1.929	-0.657
4.480	2.561	-0.685	7.656	2.881	-0.722	6.412	1.943	-0.660
4.413	2.588	-0.682	7.698	2.881	-0.722	6.330	1.958	-0.660
4.352	2.617	-0.679	7.752	2.881	-0.723	6.253	1.975	-0.660
4.300	2.648	-0.676	7.817	2.881	-0.724	6.180	1.993	-0.663
4.254	2.681	-0.674	7.894	2.881	-0.723	6.111	2.012	-0.665
4.217	2.715	-0.672	7.982	2.881	-0.724	6.048	2.033	-0.669
4.187	2.750	-0.670	8.077	2.880	-0.724	5.990	2.054	-0.672
4.165	2.787	-0.668	8.172	2.879	-0.724	5.937	2.077	-0.673
4.151	2.823	-0.667	8.266	2.876	-0.725	5.890	2.100	-0.675
4.145	2.861	-0.664	8.358	2.872	-0.727	5.848	2.124	-0.681
4.147	2.898	-0.661	8.447	2.867	-0.728	5.811	2.149	-0.683
4.157	2.936	-0.658	8.535	2.861	-0.729	5.781	2.174	-0.685
4.175	2.973	-0.656	8.620	2.853	-0.731	5.756	2.201	-0.687
4.200	3.010	-0.654	8.703	2.844	-0.732	5.737	2.227	-0.690
4.232	3.046	-0.651	8.782	2.834	-0.734	5.724	2.254	-0.693
4.271	3.082	-0.649	8.858	2.823	-0.736	5.716	2.281	-0.696
4.317	3.116	-0.647	8.931	2.811	-0.738	5.715	2.308	-0.698
4.369	3.149	-0.645	9.001	2.797	-0.739	5.719	2.335	-0.701
4.428	3.182	-0.641	9.066	2.782	-0.740	5.728	2.362	-0.703
4.492	3.212	-0.639	9.127	2.766	-0.744	5.744	2.389	-0.706
4.561	3.242	-0.636	9.185	2.749	-0.744	5.764	2.416	-0.708
4.636	3.269	-0.635	9.238	2.731	-0.748	5.790	2.443	-0.710
4.715	3.295	-0.632	9.286	2.712	-0.749	5.822	2.469	-0.712
4.797	3.320	-0.629	9.329	2.692	-0.750	5.858	2.495	-0.712
4.884	3.342	-0.624	9.368	2.671	-0.753	5.900	2.521	-0.715
4.974	3.362	-0.620	9.401	2.649	-0.756	5.946	2.546	-0.717
5.066	3.380	-0.618	9.430	2.626	-0.757	5.997	2.570	-0.718
5.160	3.397	-0.618	9.453	2.602	-0.758	6.052	2.594	-0.720
5.257	3.411	-0.616	9.470	2.577	-0.761	6.112	2.617	-0.722
5.343	3.423	-0.614	9.482	2.552	-0.762	6.176	2.639	-0.722
5.413	3.433	-0.611	9.488	2.526	-0.762	6.244	2.661	-0.722
5.466	3.440	-0.610	9.489	2.499	-0.761	6.315	2.682	-0.721
5.501	3.445	-0.610	9.484	2.472	-0.764	6.390	2.702	-0.724
5.518	3.448	-0.609	9.473	2.445	-0.763	6.468	2.721	-0.722
5.519	2.948	-0.703	9.456	2.417	-0.763	6.550	2.739	-0.721
5.547	2.948	-0.692	9.434	2.389	-0.761	6.634	2.756	-0.724
5.583	2.948	-0.692	9.406	2.361	-0.761	6.720	2.772	-0.722
5.632	2.948	-0.690	9.372	2.332	-0.761	6.809	2.787	-0.722
5.695	2.948	-0.692	9.332	2.304	-0.758	6.900	2.801	-0.721
5.771	2.943	-0.692	9.287	2.276	-0.755	6.993	2.814	-0.721
5.850	2.919	-0.698	9.236	2.248	-0.755	7.088	2.826	-0.721
5.930	2.895	-0.705	9.180	2.220	-0.752	7.183	2.837	-0.719
6.010	2.870	-0.709	9.119	2.192	-0.747	7.279	2.846	-0.721
6.090	2.846	-0.713	9.053	2.166	-0.744	7.363	2.855	-0.722
6.170	2.821	-0.715	8.982	2.139	-0.741	7.436	2.862	-0.721

7.497	2.869	-0.721
7.545	2.874	-0.721
7.579	2.877	-0.720
7.609	2.381	-0.754
7.624	2.381	-0.745
7.647	2.381	-0.743
7.681	2.381	-0.743
7.724	2.381	-0.744
7.778	2.381	-0.745
7.841	2.381	-0.745
7.914	2.381	-0.746
7.994	2.380	-0.748
8.074	2.380	-0.748
8.154	2.380	-0.750
8.234	2.380	-0.751
8.313	2.379	-0.753
8.393	2.379	-0.753
8.473	2.379	-0.753
8.553	2.378	-0.755
8.633	2.378	-0.756
8.713	2.378	-0.758
8.793	2.378	-0.758
8.873	2.377	-0.759
8.953	2.377	-0.760
9.033	2.377	-0.761
9.113	2.376	-0.761
9.193	2.376	-0.762
9.273	2.376	-0.763
9.352	2.376	-0.763
9.432	2.375	-0.764
9.512	2.375	-0.766
9.592	2.375	-0.765
9.672	2.374	-0.766
9.752	2.374	-0.767
9.832	2.374	-0.768
9.912	2.374	-0.768
9.992	2.373	-0.769
10.072	2.373	-0.770
10.152	2.373	-0.771
10.232	2.372	-0.771
10.312	2.372	-0.771
10.392	2.372	-0.771
10.471	2.372	-0.771
10.551	2.371	-0.771
10.235	2.872	-0.722
10.248	2.872	-0.724
10.271	2.872	-0.722
10.304	2.872	-0.723
10.345	2.872	-0.718
10.397	2.872	-0.718
10.456	2.872	-0.711
10.525	2.872	-0.717
10.602	2.872	-0.709
10.687	2.872	-0.713
10.780	2.872	-0.710
10.876	2.872	-0.706
10.971	2.871	-0.704
11.065	2.869	-0.692
11.158	2.867	-0.679
11.249	2.864	-0.689
11.339	2.860	-0.680
11.427	2.855	-0.676
11.514	2.850	-0.672
11.598	2.844	-0.679
11.681	2.838	-0.683
11.761	2.831	-0.681
11.840	2.823	-0.682
11.915	2.814	-0.676
11.989	2.805	-0.684
12.059	2.795	-0.675
12.127	2.785	-0.683
12.192	2.774	-0.686
12.254	2.762	-0.688
12.313	2.750	-0.690
12.368	2.737	-0.699
12.421	2.723	-0.697
12.470	2.709	-0.701
12.515	2.694	-0.706
12.557	2.679	-0.715
12.595	2.663	-0.717
12.629	2.647	-0.720
12.660	2.630	-0.728
12.686	2.613	-0.734
12.709	2.595	-0.733
12.728	2.577	-0.736
12.742	2.558	-0.739
12.752	2.539	-0.743
12.759	2.520	-0.743
12.761	2.501	-0.744
12.758	2.481	-0.747
12.752	2.460	-0.747
12.741	2.440	-0.748
12.725	2.419	-0.749
12.706	2.398	-0.750
12.682	2.378	-0.751
12.654	2.357	-0.751
12.622	2.335	-0.752
12.585	2.314	-0.751
12.544	2.293	-0.753
12.499	2.272	-0.752
12.450	2.251	-0.752
12.397	2.230	-0.751
12.340	2.210	-0.751
12.279	2.189	-0.750
12.214	2.169	-0.750
12.146	2.150	-0.749
12.074	2.130	-0.748
11.999	2.111	-0.746
11.920	2.093	-0.744
11.838	2.074	-0.742
11.753	2.057	-0.740
11.665	2.040	-0.736
11.574	2.024	-0.736
11.481	2.008	-0.734
11.386	1.993	-0.732
11.288	1.979	-0.729
11.188	1.965	-0.726
11.086	1.953	-0.724
10.982	1.941	-0.721
10.877	1.930	-0.718
10.771	1.920	-0.718
10.664	1.911	-0.714
10.556	1.902	-0.713
10.447	1.895	-0.711
10.338	1.889	-0.708
10.228	1.884	-0.707
10.118	1.879	-0.705
10.009	1.876	-0.703
9.900	1.874	-0.701
9.792	1.873	-0.698
9.685	1.872	-0.697
9.578	1.873	-0.695
9.473	1.875	-0.694
9.369	1.878	-0.693
9.267	1.882	-0.692
9.167	1.887	-0.692
9.069	1.893	-0.694
8.973	1.900	-0.694
8.880	1.907	-0.693
8.789	1.916	-0.693
8.701	1.925	-0.694
8.615	1.936	-0.695
8.533	1.947	-0.697
8.454	1.959	-0.699
8.378	1.972	-0.702
8.306	1.985	-0.705
8.237	2.000	-0.703
8.172	2.015	-0.704
8.111	2.030	-0.706
8.054	2.046	-0.706
8.000	2.063	-0.707
7.951	2.080	-0.709
7.905	2.098	-0.709
7.864	2.116	-0.713
7.827	2.134	-0.716
7.794	2.153	-0.719
7.765	2.172	-0.720
7.741	2.191	-0.720
7.721	2.211	-0.723
7.706	2.231	-0.724
7.694	2.251	-0.726
7.687	2.271	-0.728
7.684	2.291	-0.730
7.686	2.311	-0.733
7.692	2.331	-0.735
7.701	2.352	-0.736
7.715	2.372	-0.737
7.734	2.392	-0.738
7.756	2.412	-0.741
7.782	2.432	-0.741
7.812	2.451	-0.742
7.846	2.471	-0.745
7.884	2.490	-0.745
7.925	2.509	-0.746
7.970	2.528	-0.746
8.019	2.546	-0.747
8.071	2.564	-0.747
8.126	2.582	-0.747
8.185	2.599	-0.748
8.246	2.616	-0.748
8.311	2.633	-0.748
8.379	2.649	-0.749
8.449	2.665	-0.748
8.522	2.680	-0.748
8.597	2.694	-0.747
8.675	2.709	-0.746
8.756	2.722	-0.746
8.838	2.735	-0.746
8.922	2.748	-0.745
9.009	2.760	-0.746
9.097	2.772	-0.744
9.187	2.783	-0.744
9.278	2.793	-0.742
9.370	2.803	-0.742
9.464	2.812	-0.742
9.559	2.820	-0.740
9.655	2.828	-0.738
9.752	2.836	-0.736
9.841	2.842	-0.733
9.922	2.848	-0.730
9.994	2.854	-0.726
10.057	2.859	-0.723
10.111	2.863	-0.723
10.155	2.866	-0.721
10.189	2.869	-0.719
10.213	2.871	-0.721
10.227	2.872	-0.718
10.232	2.372	-0.767

Optimization Run #2

Table S10. Tabulated data from the second optimization run starting at $[\tau, \text{Equiv}]_0 = [15 \text{ min}, 3.5]$

Tau (min)	Eq (-)	Obj Func (-)
15.000	4.000	0.677
15.005	4.000	0.676
15.017	4.000	0.676
15.036	4.000	0.675
15.061	4.000	0.679
15.093	4.000	0.678
15.131	4.000	0.681
15.175	4.000	0.683
15.226	4.000	0.686
15.283	4.000	0.688
15.346	4.000	0.691
15.415	4.000	0.694
15.489	4.000	0.699
15.569	4.000	0.701
15.654	4.000	0.705
15.745	4.000	0.709
15.841	4.000	0.714
15.937	4.000	0.719
16.032	3.999	0.723
16.126	3.998	0.728
16.220	3.997	0.734
16.313	3.995	0.737
16.405	3.993	0.741
16.497	3.991	0.745
16.587	3.989	0.749
16.676	3.986	0.753
16.764	3.983	0.758
16.850	3.979	0.761
16.936	3.975	0.765
17.020	3.971	0.767
17.102	3.967	0.771
17.184	3.962	0.772
17.263	3.957	0.775
17.341	3.952	0.777
17.418	3.946	0.782
17.493	3.940	0.783
17.566	3.934	0.785
17.637	3.927	0.787
17.707	3.920	0.790
17.774	3.913	0.790
17.840	3.906	0.792
17.903	3.898	0.792
17.965	3.890	0.793
18.024	3.881	0.794
18.081	3.873	0.794
18.136	3.864	0.795
18.189	3.854	0.796
18.239	3.845	0.795
18.287	3.835	0.794
18.333	3.825	0.793
18.376	3.815	0.792
18.417	3.805	0.793
18.455	3.794	0.791
18.491	3.783	0.789
18.524	3.772	0.788
18.554	3.760	0.785
18.582	3.748	0.782
18.607	3.736	0.598
18.629	3.724	0.777
18.649	3.712	0.773
18.666	3.700	0.769
18.680	3.687	0.765
18.691	3.674	0.762
18.699	3.661	0.760
18.705	3.648	0.755
18.707	3.634	0.751
18.707	3.621	0.746
18.704	3.607	0.740
18.697	3.593	0.736
18.688	3.580	0.731
18.676	3.566	0.725
18.661	3.551	0.719
18.643	3.537	0.712
18.623	3.523	0.706
18.599	3.509	0.700
18.572	3.494	0.693
18.543	3.480	0.687
18.510	3.466	0.679
18.475	3.451	0.673
18.436	3.437	0.666
18.395	3.423	0.659
18.351	3.408	0.650
18.304	3.394	0.643
18.255	3.380	0.637
18.203	3.365	0.628
18.147	3.351	0.621
18.090	3.337	0.611
18.029	3.323	0.603
17.966	3.309	0.597
17.901	3.296	0.589
17.833	3.282	0.580
17.763	3.269	0.572
17.690	3.256	0.563
17.614	3.243	0.555
17.537	3.230	0.546
17.457	3.217	0.539
17.375	3.205	0.530
17.291	3.193	0.522
17.205	3.181	0.515
17.117	3.170	0.506
17.027	3.158	0.498
16.936	3.147	0.491
16.842	3.137	0.483
16.747	3.126	0.473
16.650	3.116	0.466
16.552	3.107	0.459
16.453	3.097	0.451
16.352	3.089	0.444
16.250	3.080	0.437
16.146	3.072	0.429
16.042	3.064	0.423
15.937	3.057	0.416
15.831	3.050	0.410
15.724	3.043	0.403
15.616	3.037	0.395
15.508	3.032	0.390
15.399	3.026	0.384
15.290	3.022	0.364
15.181	3.017	0.338
15.072	3.014	0.297
14.962	3.010	0.256
14.853	3.007	0.283
14.743	3.005	0.229
14.634	3.003	0.190
14.525	3.002	0.174
14.417	3.001	0.153
14.309	3.000	0.148
14.201	3.000	0.102
14.095	3.001	0.053
13.989	3.001	0.053
13.884	3.003	0.084
13.780	3.005	0.029
13.678	3.007	-0.006
13.576	3.010	-0.016
13.476	3.013	-0.003
13.377	3.017	-0.048
13.279	3.021	-0.054
13.183	3.026	-0.045
13.089	3.031	-0.030
12.996	3.036	-0.063
12.905	3.042	-0.053
12.816	3.048	-0.089
12.729	3.055	-0.053
12.644	3.062	-0.046
12.561	3.070	-0.059
12.480	3.078	-0.041
12.401	3.086	-0.041
12.325	3.095	-0.035
12.250	3.104	-0.036
12.179	3.113	-0.040
12.109	3.122	-0.050
12.042	3.132	-0.058
11.978	3.143	-0.042
11.916	3.153	-0.039
11.857	3.164	-0.030
11.801	3.175	-0.016
11.747	3.186	-0.004
11.696	3.198	-0.003
11.647	3.210	0.047
11.602	3.222	0.026
11.559	3.234	0.038
11.519	3.246	0.067
11.482	3.259	0.063
11.448	3.272	0.091
11.417	3.285	0.113
11.388	3.298	0.145
11.363	3.311	0.123
11.341	3.324	0.196
11.321	3.337	0.209
11.304	3.351	0.228
11.291	3.365	0.229
11.280	3.378	0.294
11.272	3.392	0.310
11.267	3.406	0.322
11.265	3.419	0.367
11.266	3.433	0.372
11.270	3.447	0.376
11.277	3.461	0.380
11.287	3.475	0.383
11.299	3.488	0.388
11.314	3.502	0.392
11.332	3.516	0.396

11.353	3.529	0.402	14.793	3.500	0.486	9.171	2.713	-0.745
11.377	3.543	0.406	14.740	3.500	0.484	9.084	2.700	-0.748
11.403	3.557	0.411	14.681	3.500	0.482	8.997	2.687	-0.755
11.432	3.570	0.415	14.616	3.500	0.478	8.910	2.674	-0.766
11.464	3.583	0.422	14.545	3.500	0.475	8.823	2.661	-0.766
11.498	3.597	0.424	14.467	3.500	0.472	8.736	2.648	-0.770
11.535	3.610	0.429	14.383	3.499	0.469	8.650	2.635	-0.774
11.574	3.623	0.436	14.296	3.486	0.463	8.563	2.622	-0.776
11.616	3.636	0.441	14.209	3.472	0.455	8.476	2.609	-0.777
11.660	3.649	0.445	14.122	3.459	0.447	8.389	2.596	-0.779
11.707	3.661	0.451	14.035	3.446	0.441	8.302	2.582	-0.779
11.756	3.674	0.455	13.949	3.433	0.435	8.215	2.569	-0.780
11.807	3.686	0.461	13.862	3.420	0.429	8.128	2.556	-0.779
11.861	3.698	0.466	13.775	3.407	0.419	8.042	2.543	-0.777
11.917	3.710	0.471	13.688	3.394	0.414	8.220	3.069	-0.591
11.975	3.722	0.476	13.601	3.381	0.409	8.237	3.069	-0.589
12.035	3.734	0.482	13.514	3.368	0.401	8.266	3.069	-0.585
12.098	3.745	0.487	13.427	3.355	0.395	8.306	3.069	-0.576
12.162	3.757	0.494	13.340	3.342	0.389	8.358	3.069	-0.574
12.229	3.768	0.499	13.254	3.328	0.384	8.421	3.069	-0.582
12.297	3.779	0.503	13.167	3.315	0.377	8.495	3.069	-0.586
12.367	3.789	0.508	13.080	3.302	0.371	8.579	3.069	-0.569
12.439	3.800	0.513	12.993	3.289	0.365	8.672	3.069	-0.578
12.513	3.810	0.519	12.906	3.276	0.361	8.768	3.069	-0.582
12.589	3.820	0.525	12.819	3.263	0.354	8.862	3.067	-0.569
12.666	3.830	0.531	12.732	3.250	0.348	8.955	3.064	-0.579
12.745	3.839	0.536	12.646	3.237	0.342	9.047	3.060	-0.547
12.825	3.849	0.542	12.559	3.224	0.339	9.136	3.055	-0.551
12.907	3.858	0.547	12.472	3.211	0.300	9.223	3.049	-0.556
12.990	3.867	0.553	12.385	3.198	0.240	9.308	3.042	-0.563
13.075	3.875	0.559	12.298	3.185	0.242	9.391	3.034	-0.562
13.161	3.883	0.564	12.211	3.171	0.170	9.471	3.025	-0.564
13.248	3.892	0.570	12.124	3.158	0.102	9.547	3.014	-0.569
13.337	3.899	0.575	12.037	3.145	0.053	9.621	3.003	-0.567
13.426	3.907	0.581	11.951	3.132	-0.016	9.692	2.991	-0.541
13.517	3.914	0.586	11.864	3.119	-0.015	9.759	2.977	-0.577
13.608	3.921	0.592	11.777	3.106	-0.026	9.822	2.963	-0.570
13.701	3.928	0.598	11.690	3.093	-0.090	9.882	2.948	-0.572
13.794	3.934	0.604	11.603	3.080	-0.133	9.937	2.932	-0.584
13.888	3.940	0.610	11.516	3.067	-0.222	9.989	2.915	-0.595
13.983	3.946	0.615	11.429	3.054	-0.215	10.036	2.897	-0.617
14.079	3.952	0.621	11.343	3.041	-0.238	10.078	2.878	-0.627
14.175	3.957	0.626	11.256	3.027	-0.304	10.116	2.858	-0.623
14.272	3.962	0.633	11.169	3.014	-0.334	10.150	2.838	-0.631
14.364	3.967	0.638	11.082	3.001	-0.347	10.178	2.817	-0.646
14.451	3.971	0.643	10.995	2.988	-0.406	10.202	2.795	-0.656
14.532	3.975	0.649	10.908	2.975	-0.410	10.221	2.772	-0.676
14.607	3.979	0.652	10.821	2.962	-0.438	10.234	2.749	-0.685
14.675	3.983	0.656	10.734	2.949	-0.455	10.243	2.725	-0.696
14.737	3.986	0.660	10.648	2.936	-0.470	10.246	2.701	-0.714
14.793	3.989	0.665	10.561	2.923	-0.501	10.244	2.676	-0.729
14.842	3.991	0.668	10.474	2.910	-0.550	10.236	2.651	-0.732
14.885	3.994	0.670	10.387	2.897	-0.553	10.223	2.625	-0.751
14.921	3.996	0.673	10.300	2.883	-0.590	10.205	2.599	-0.756
14.950	3.997	0.675	10.213	2.870	-0.596	10.181	2.573	-0.769
14.973	3.999	0.676	10.126	2.857	-0.618	10.152	2.547	-0.783
14.989	3.999	0.679	10.039	2.844	-0.626	10.118	2.521	-0.784
14.998	4.000	0.677	9.953	2.831	-0.654	10.078	2.494	-0.790
15.000	3.500	0.495	9.866	2.818	-0.661	10.034	2.468	-0.792
14.994	3.500	0.493	9.779	2.805	-0.672	9.984	2.442	-0.793
14.982	3.500	0.494	9.692	2.792	-0.694	9.929	2.416	-0.796
14.966	3.500	0.491	9.605	2.779	-0.708	9.870	2.391	-0.793
14.943	3.500	0.491	9.518	2.766	-0.703	9.805	2.366	-0.793
14.914	3.500	0.490	9.431	2.753	-0.714	9.736	2.341	-0.792
14.880	3.500	0.489	9.345	2.740	-0.732	9.663	2.317	-0.790
14.839	3.500	0.487	9.258	2.726	-0.736	9.585	2.294	-0.788

9.504	2.271	-0.786	7.392	2.982	-0.707	12.313	2.172	-0.779
9.418	2.249	-0.783	7.484	2.995	-0.696	12.273	2.150	-0.777
9.329	2.229	-0.780	7.577	3.006	-0.675	12.229	2.129	-0.775
9.237	2.209	-0.776	7.672	3.017	-0.679	12.180	2.107	-0.775
9.142	2.190	-0.774	7.768	3.027	-0.670	12.127	2.086	-0.773
9.044	2.172	-0.771	7.863	3.036	-0.660	12.070	2.065	-0.770
8.943	2.156	-0.766	7.947	3.044	-0.642	12.009	2.044	-0.767
8.840	2.141	-0.764	8.021	3.051	-0.648	11.945	2.024	-0.763
8.735	2.127	-0.760	8.083	3.056	-0.633	11.876	2.003	-0.763
8.629	2.115	-0.758	8.134	3.061	-0.618	11.804	1.984	-0.759
8.521	2.104	-0.754	8.173	3.065	-0.624	11.729	1.964	-0.756
8.413	2.094	-0.751	8.199	3.068	-0.606	11.650	1.945	-0.752
8.304	2.086	-0.748	8.213	3.069	-0.612	11.567	1.927	-0.750
8.194	2.080	-0.744	8.215	2.569	-0.774	11.482	1.909	-0.747
8.085	2.075	-0.741	10.007	2.727	-0.724	11.394	1.892	-0.743
7.975	2.071	-0.740	10.017	2.727	-0.727	11.303	1.875	-0.738
7.867	2.070	-0.737	10.038	2.727	-0.717	11.209	1.859	-0.736
7.760	2.070	-0.734	10.068	2.727	-0.730	11.113	1.844	-0.733
7.654	2.071	-0.733	10.107	2.727	-0.713	11.014	1.830	-0.729
7.549	2.074	-0.730	10.156	2.727	-0.720	10.914	1.816	-0.724
7.447	2.079	-0.731	10.214	2.727	-0.710	10.812	1.803	-0.722
7.347	2.085	-0.728	10.282	2.727	-0.721	10.708	1.792	-0.716
7.250	2.092	-0.730	10.357	2.727	-0.703	10.602	1.781	-0.713
7.155	2.102	-0.729	10.441	2.727	-0.709	10.495	1.771	-0.711
7.063	2.112	-0.727	10.533	2.727	-0.698	10.388	1.762	-0.707
6.975	2.124	-0.728	10.629	2.727	-0.687	10.279	1.754	-0.703
6.891	2.137	-0.727	10.724	2.726	-0.685	10.170	1.747	-0.701
6.810	2.152	-0.727	10.818	2.724	-0.695	10.061	1.741	-0.697
6.734	2.168	-0.728	10.911	2.721	-0.680	9.951	1.736	-0.695
6.662	2.184	-0.728	11.003	2.718	-0.673	9.842	1.732	-0.691
6.594	2.202	-0.730	11.092	2.714	-0.685	9.733	1.729	-0.690
6.531	2.221	-0.731	11.181	2.710	-0.676	9.624	1.728	-0.687
6.472	2.241	-0.733	11.267	2.704	-0.672	9.516	1.727	-0.684
6.419	2.262	-0.733	11.351	2.698	-0.661	9.410	1.727	-0.683
6.370	2.283	-0.734	11.434	2.692	-0.674	9.304	1.729	-0.682
6.327	2.306	-0.736	11.514	2.684	-0.668	9.200	1.731	-0.681
6.289	2.328	-0.737	11.592	2.676	-0.684	9.097	1.735	-0.681
6.256	2.352	-0.737	11.667	2.667	-0.671	8.996	1.740	-0.680
6.228	2.376	-0.740	11.740	2.658	-0.658	8.898	1.745	-0.679
6.206	2.400	-0.741	11.810	2.647	-0.677	8.801	1.752	-0.678
6.189	2.424	-0.741	11.877	2.637	-0.673	8.707	1.760	-0.678
6.177	2.449	-0.742	11.941	2.625	-0.680	8.615	1.768	-0.680
6.171	2.474	-0.742	12.002	2.613	-0.694	8.527	1.778	-0.681
6.170	2.500	-0.744	12.060	2.600	-0.681	8.441	1.788	-0.681
6.175	2.525	-0.744	12.114	2.586	-0.688	8.358	1.800	-0.683
6.184	2.550	-0.746	12.165	2.572	-0.688	8.278	1.812	-0.683
6.199	2.575	-0.746	12.213	2.558	-0.702	8.202	1.825	-0.685
6.219	2.600	-0.746	12.257	2.542	-0.702	8.130	1.839	-0.688
6.244	2.625	-0.746	12.297	2.527	-0.708	8.060	1.853	-0.688
6.274	2.649	-0.746	12.334	2.510	-0.717	7.995	1.868	-0.691
6.308	2.674	-0.745	12.366	2.493	-0.723	7.934	1.884	-0.693
6.348	2.697	-0.746	12.395	2.476	-0.732	7.876	1.901	-0.695
6.391	2.721	-0.746	12.419	2.458	-0.740	7.823	1.918	-0.699
6.440	2.744	-0.745	12.440	2.440	-0.739	7.773	1.935	-0.701
6.492	2.766	-0.745	12.456	2.421	-0.755	7.728	1.953	-0.704
6.549	2.788	-0.744	12.468	2.402	-0.758	7.687	1.972	-0.707
6.609	2.809	-0.743	12.476	2.382	-0.762	7.651	1.991	-0.710
6.673	2.830	-0.742	12.479	2.362	-0.760	7.618	2.010	-0.713
6.741	2.850	-0.739	12.478	2.342	-0.768	7.590	2.029	-0.717
6.813	2.869	-0.738	12.473	2.321	-0.773	7.567	2.049	-0.721
6.887	2.888	-0.736	12.463	2.300	-0.777	7.548	2.069	-0.724
6.965	2.905	-0.731	12.449	2.279	-0.778	7.533	2.090	-0.726
7.045	2.922	-0.729	12.431	2.258	-0.779	7.523	2.110	-0.730
7.129	2.939	-0.724	12.408	2.237	-0.781	7.517	2.131	-0.733
7.214	2.954	-0.718	12.381	2.215	-0.782	7.515	2.151	-0.735
7.302	2.968	-0.715	12.349	2.194	-0.781	7.518	2.172	-0.739

7.525	2.193	-0.742
7.536	2.213	-0.745
7.552	2.234	-0.747
7.572	2.255	-0.750
7.595	2.275	-0.752
7.623	2.295	-0.755
7.655	2.315	-0.757
7.691	2.335	-0.759
7.731	2.354	-0.761
7.774	2.374	-0.762
7.821	2.393	-0.765
7.871	2.411	-0.767
7.925	2.430	-0.767
7.983	2.447	-0.769
8.043	2.465	-0.771
8.107	2.482	-0.771
8.174	2.499	-0.772
8.243	2.515	-0.773
8.315	2.530	-0.772
8.390	2.545	-0.774
8.468	2.560	-0.775
8.547	2.574	-0.776
8.629	2.588	-0.776
8.714	2.601	-0.776
8.800	2.613	-0.774
8.888	2.625	-0.773
8.977	2.636	-0.768
9.068	2.647	-0.764
9.161	2.657	-0.770
9.255	2.666	-0.762
9.350	2.675	-0.758
9.446	2.683	-0.750
9.542	2.690	-0.744
9.631	2.697	-0.750
9.711	2.703	-0.736
9.782	2.709	-0.737
9.844	2.714	-0.735
9.896	2.718	-0.727
9.938	2.721	-0.723
9.970	2.724	-0.716
9.992	2.726	-0.727
10.004	2.727	-0.714
10.006	2.227	-0.780

[1] Wyvratt, B. M.; McMullen, J. P.; Grosser. S. T., Multidimensional dynamic experiments for data-rich process development of reactions in flow, *Reaction Chemistry & Engineering*, **2019**, *4*, 1637-1645.

[2] Moore, J. S.; Jensen, K. F., "Batch" Kinetics in Flow: Online IR Analysis and Continuous Control. *Angewandte Chemie International Edition* **2014,** *53*, 470-473.

[3] Mozharov, S.; Nordon, A.; Littlejohn, D.; Wiles, C.; Watts, P.; Dallin, P.; Girkin, J. M., Improved Method for Kinetic Studies in Microreactors Using Flow Manipulation and Noninvasive Raman Spectrometry. *Journal of the American Chemical Society* **2011,** *133*, 3601-3608.